4. Discussion

It is well known that both macroangiopathy and microangiopathy tend to develop rapidly in patients with poorly controlled diabetes. Numerous factors present in macroangiopathy and microangiopathy such as hypertension [18,19], hyperglycemia [20], hyperinsulinemia [21,22], hyperlipidemia [7,23], oxidative stress [24,25] and so on, contribute to angiopathic progression via independent and/or coordinated mechanisms [6,21,24]. Some of these numerous effects act directly on vascular cells [26], while others affect macrophages which invade vascular cells [6]. In this study, we focused on foam cell formation from macrophages, and the activities of patient sera which induce foam cell differentiation were measured. The sera were obtained from diabetic patients, because atherosclerosis and microangiopathy develop rapidly in this patient population. To obtain reproducible values, we used the J774.1 cell line which firmly attaches to culture-dishes and changes into foam cells in response to WHHLMI rabbit serum. Assay reproducibility and validity were confirmed from intra-assay and inter-assay CVs. However, as CVs were still somewhat high, cautious cell handling is critical before proceeding to clinical use. Moreover, by GC analysis, lipid accumulation including cholesteryl ester accumulation rose in proportion to the MMI increase. No specific GC peak corresponding to MMI was detectable. Therefore, the AdipoRed assay precisely reflects intracellular lipid ester accumulation. The obtained values were thus used for comparisons with various clinical factors.

MMI was revealed to be clustered with TG and diabetic nephropathy, the latter being a well-known cause of hypertriglyceridemia [27]. Furthermore, diabetic retinopathy was relatively closely related to MMI and was presumed to be an event preceding nephropathy. Among partial coefficients of regression, age was negative and significant, in fact dovetailing with newly progressive retinopathy being less severe in elderly patients [28].

In multiple regression analysis, we selected six variables which rather strongly accounted for MMI. TG itself is thought to be the primary material of intra-TG accumulation. TZDs might have direct effects against macrophages, while with diabetic retinopathy and nephropathy, administration of an α-GI, which is minimally absorbed from the intestinal tract, and a high BMI reflect only the clinical state and are not directly related to serum parameters. Among these, α-GIs improve blood sugar fluctuations, and a high BMI (obesity) is known to produce metabolic syndrome, the major cause of insulin resistance and atherosclerotic angiopathy. From this viewpoint, it is reasonable that TZDs suppress the ill effects of obesity, by improving insulin resistance. To develop a practical assay, the system shown in the Supple. 3 Table might be worthwhile. It might actually be the case that numerous pathways and bioactive substances affect macrophage maturation in the absence of any lipid effect. Logistic regression analysis, conversely, revealed MMI to be useful for measuring the activity or progression of diabetic angiopathy. In other words, macrophage foam cell formation was related to the development of diabetic microangiopathy. At a minimum, active retinopathy and nephropathy at stage 3a or later were predictable from a higher MMI value at the same time point. Retinopathy and nephropathy acted simply in an additive manner with MMI, suggesting that a higher number of complications reflect the strength of macrophage activity.

Several clinical studies have focused on diabetic angiopathy and medications, with subsets of drugs proving to be effective against angiopathy, though the underlying mechanisms remain uncertain. The α-GIs and TZDs were demonstrated to be effective for the prevention of macrovascular diseases in the stop-NIDDM trial [29] and the PROactive study [30], respectively. However, whether or not this is attributable to direct and/or indirect effects on atherosclerotic regions rather than glycemic control remains unclear. Taking the results of this assay into consideration, these medications may function to prevent macrophage foaming. Moreover, we found that MMI reflected several factors, including foaming or lipid accumulation in individual cells, as well as cell viability and/or growth. Intensive studies focusing on both the characteristics of serum, *i.e.* analysis by 2-DE/mass spectrometry, and the corresponding effects on macrophages, *i.e.* microarray investigations, might clarify the features of macrophage activation.

This study was cross-sectional, such that relationships among variables were ambiguous in terms of cause and effect, especially the impacts of medical therapy. Most of the diabetic patients examined had already received interventional therapies including not only anti-hyperglycemic agents, but also anti-hypertensive agents, statins, anti-coagulants, and so on. Although a future intensive cohort study is needed, MMI might be corrected to avoid excessively strong effects of the lipid state, thus truly reflecting the risk of developing angiopathic diseases in patients with Type 2 diabetes, and thereby become a useful indicator for selecting appropriate medical therapy.

Acknowledgements

We are deeply grateful to Hirokazu Sato and Yuko Oki for their technical supports. This work was supported by a Grant-in-Aid for Exploratory Research from the Japan Promotion of Science Foundation of the Japanese Government.

Appendix A. Supplementary data

Supplementary data associated with this article can be found, in the online version, at doi:10.1016/j.diabres.2009.10.011.

Conflict of interest

There are no conflicts of interest.

REFERENCES

[1] Tesch, Role of macrophages in complications of type 2 diabetes, Clin. Exp. Pharmacol. Physiol. 34 (2007) 1016–1019.
[2] Nguyen, Ping, Mu, Hill, Atkins, Chadban, Macrophage accumulation in human progressive diabetic nephropathy, Nephrology (Carlton) 11 (2006) 226–231.

[3] Boyle, Diabetes mellitus and macrovascular disease: mechanisms and mediators, Am. J. Med. 120 (2007) S12–17.
[4] Simionescu, Implications of early structural-functional changes in the endothelium for vascular disease, Arterioscler. Thromb. Vasc. Biol. 27 (2007) 266–274.
[5] Gacka, Dobosz, Szymaniec, Bednarska-Chabowska, Adamiec, Sadakierska-Chudy, Proinflammatory and atherogenic activity of monocytes in Type 2 diabetes, J. Diabetes Complications (2008).
[6] Hodgkinson, Laxton, Patel, Ye, Advanced glycation end-product of low density lipoprotein activates the toll-like 4 receptor pathway implications for diabetic atherosclerosis, Arterioscler. Thromb. Vasc. Biol. 28 (2008) 2275–2281.
[7] Ishigaki, Katagiri, Gao, Yamada, Imai, Uno, et al., Impact of plasma oxidized low-density lipoprotein removal on atherosclerosis, Circulation 118 (2008) 75–83.
[8] Mori, Itabe, Higashi, Fujimoto, Shiomi, Yoshizumi, et al., Foam cell formation containing lipid droplets enriched with free cholesterol by hyperlipidemic serum, J. Lipid Res. 42 (2001) 1771–1781.
[9] Shiomi, Ito, Yamada, Kawashima, Fan, Development of an animal model for spontaneous myocardial infarction (WHHLMI rabbit), Arterioscler. Thromb. Vasc. Biol. 23 (2003) 1239–1244.
[10] Tanzawa, Shimada, Kuroda, Tsujita, Arai, Watanabe, WHHL-rabbit: a low density lipoprotein receptor-deficient animal model for familial hypercholesterolemia, FEBS Lett. 118 (1980) 81–84.
[11] Buja, Kita, Goldstein, Watanabe, Brown, Cellular pathology of progressive atherosclerosis in the WHHL rabbit. An animal model of familial hypercholesterolemia, Arteriosclerosis 3 (1983) 87–101.
[12] Shiomi, Ito, Shiraishi, Watanabe, Inheritability of atherosclerosis and the role of lipoproteins as risk factors in the development of atherosclerosis in WHHL rabbits: risk factors related to coronary atherosclerosis are different from those related to aortic atherosclerosis, Atherosclerosis 96 (1992) 43–52.
[13] Ishii, Kita, Yokode, Kume, Nagano, Otani, et al., Characterization of very low density lipoprotein from Watanabe heritable hyperlipidemic rabbits, J. Lipid Res. 30 (1989) 1–7.
[14] Ito, Yamada, Shiomi, Progression of coronary atherosclerosis relates to the onset of myocardial infarction in an animal model of spontaneous myocardial infarction (WHHLMI rabbits), Exp. Anim. 53 (2004) 339–346.
[15] Greenspan, Fowler, Spectrofluorometric studies of the lipid probe, nile red, J. Lipid Res. 26 (1985) 781–789.
[16] Kushiyama, Shojima, Ogihara, Inukai, Sakoda, Fujishiro, et al., Resistin-like molecule beta activates MAPKs, suppresses insulin signaling in hepatocytes, and induces diabetes, hyperlipidemia, and fatty liver in transgenic mice on a high fat diet, J. Biol. Chem. 280 (2005) 42016–42025.
[17] Fukuda, Classification and treatment of diabetic retinopathy, Diabetes Res. Clin. Pract. 24 Suppl. (1994) S171–176.
[18] Veglio, Paglieri, Rabbia, Bisbocci, Bergui, Cerrato, Hypertension and cerebrovascular damage, Atherosclerosis (2008).
[19] Silva, Pinto, Biswas, de Faria, de Faria, Hypertension increases retinal inflammation in experimental diabetes: a possible mechanism for aggravation of diabetic retinopathy by hypertension, Curr. Eye Res. 32 (2007) 533–541.
[20] Avogaro, de Kreutzenberg, Fadini, Endothelial dysfunction: causes and consequences in patients with diabetes mellitus, Diabetes Res. Clin. Pract. 82 Suppl. 2 (2008) S94–S101.
[21] Vaidyula, Boden, Rao, Platelet and monocyte activation by hyperglycemia and hyperinsulinemia in healthy subjects, Platelets 17 (2006) 577–585.
[22] Sugimoto, Baba, Suda, Yasujima, Yagihashi, Peripheral neuropathy and microangiopathy in rats with insulinoma: association with chronic hyperinsulinemia, Diabetes Metab. Res. Rev. 19 (2003) 392–400.
[23] Yang, Shi, Hao, Li, Le, Increasing oxidative stress with progressive hyperlipidemia in human: relation between malondialdehyde and atherogenic index, J. Clin. Biochem. Nutr. 43 (2008) 154–158.
[24] Ogihara, Asano, Katagiri, Sakoda, Anai, Shojima, et al., Oxidative stress induces insulin resistance by activating the nuclear factor-kappa B pathway and disrupting normal subcellular distribution of phosphatidylinositol 3-kinase, Diabetologia 47 (2004) 794–805.
[25] Osto, Matter, Kouroedov, Malinski, Bachschmid, Camici, et al., c-Jun N-terminal kinase 2 deficiency protects against hypercholesterolemia-induced endothelial dysfunction and oxidative stress, Circulation 118 (2008) 2073–2080.
[26] Kakehashi, Inoda, Mameuda, Kuroki, Jono, Nagai, et al., Relationship among VEGF, VEGF receptor, AGEs, and macrophages in proliferative diabetic retinopathy, Diabetes Res. Clin. Pract. 79 (2008) 438–445.
[27] Yoshino, Hirano, Nagata, Maeda, Naka, Murata, et al., Hypertriglyceridemia in nephrotic rats is due to a clearance defect of plasma triglyceride: overproduction of triglyceride-rich lipoprotein is not an obligatory factor, J. Lipid Res. 34 (1993) 875–884.
[28] Wong, Molyneaux, Constantino, Twigg, Yue, Timing is everything: age of onset influences long-term retinopathy risk in type 2 diabetes, independent of traditional risk factors, Diabetes Care 31 (2008) 1985–1990.
[29] Chiasson, Josse, Gomis, Hanefeld, Karasik, Laakso, Acarbose for prevention of type 2 diabetes mellitus: the STOP-NIDDM randomised trial, Lancet 359 (2002) 2072–2077.
[30] PROactive study, Lancet 367 (2006) 982.

Inhibition of endothelial cell activation by bHLH protein E2-2 and its impairment of angiogenesis

Aya Tanaka,[1] Fumiko Itoh,[1] Koichi Nishiyama,[2] Toshiaki Takezawa,[3] Hiroki Kurihara,[2] Susumu Itoh,[1] and Mitsuyasu Kato[1]

[1]Department of Experimental Pathology, Graduate School of Comprehensive Human Sciences, University of Tsukuba, Tsukuba; [2]Department of Physiological Chemistry and Metabolism, Graduate School of Medicine, University of Tokyo, Tokyo; and [3]Transgenic Animal Research Center, National Institute of Agrobiological Sciences, Tsukuba, Japan

E2-2 **belongs to the basic helix-loop-helix (bHLH) family of transcription factors. E2-2 associates with inhibitor of DNA binding (Id) 1, which is involved in angiogenesis. In this paper, we demonstrate that E2-2 interacts with Id1 and provide evidence that this interaction potentiates angiogenesis. Mutational analysis revealed that the HLH domain of E2-2 is required for the interaction with Id1 and vice versa. In addition, Id1 interfered with E2-2–mediated effects on luciferase reporter activities. Interestingly, injection of E2-2–expressing adenoviruses into Matrigel plugs implanted under the skin blocked in vivo angiogenesis. In contrast, the injection of Id1-expressing adenoviruses rescued E2-2–mediated inhibition of in vivo angiogenic reaction. Consistent with the results of the Matrigel plug assay, E2-2 could inhibit endothelial cell (EC) migration, network formation, and proliferation. On the other hand, knockdown of E2-2 in ECs increased EC migration. The blockade of EC migration by E2-2 was relieved by exogenous expression of Id1. We also demonstrated that E2-2 can perturb VEGFR2 expression via inhibition of VEGFR2 promoter activity. This study suggests that E2-2 can maintain EC quiescence and that Id1 can counter this effect. (*Blood*. 2010;115(20): 4138-4147)**

Introduction

Angiogenesis is the formation of new vessels from preexisting ones by sprouting or by intussusceptive microvascular growth. Angiogenesis takes place throughout development as well as in adulthood. Although the vasculature in adults is generally quiescent, angiogenesis occurs to ensure physiologic homeostasis and integrity after wound healing, inflammation, ischemia, and during the female reproductive cycle.[1] Angiogenesis encompasses 2 phases: activation and resolution. The activation phase is initiated by growth factor signals (eg, vascular endothelial growth factor [VEGF], fibroblast growth factor-2 [FGF-2]) or by hypoxia. In this process, endothelial cells (ECs) proliferate, vascular permeability increases, and extracellular matrix components are degraded. These serial events allow ECs to migrate and form new capillary sprouts. During the resolution stage, ECs cease proliferation and migration, the basement membrane is reconstituted, and the vessels mature. The transition from the activation phase to the resolution phase, and vice versa, is referred to as the "angiogenic switch" and is determined by a tightly regulated balance between angiogenic inducers and inhibitors.[2]

The inhibitor of the DNA-binding (Id) family of proteins, consisting of *Id1*, *Id2*, *Id3*, and *Id4*, belongs to the helix-loop-helix (HLH) family of transcription factors. The basic HLH (bHLH) family of transcription factors regulates transcription by binding to DNA as either homodimers or heterodimers. Id proteins, which lack a DNA-binding domain, interact with bHLH proteins to prevent dimer formation and/or DNA binding.[3] In addition, Id1 can associate with members of the Ets protein family and Rb.[4,5] Several observations support a crucial role for Id proteins in development, differentiation, and proliferation of cells, and in tumorigenesis. For example, it has been demonstrated that Id1 can block MyoD-mediated myogenic responses.[6-8] *Id1* and *Id3*, identified as direct targets of bone morphogenetic protein (BMP) signaling,[9-15] are abundantly expressed during blood vessel formation. *Id1/Id3* double-knockout mice display abnormal angiogenesis characterized by enlarged, dilated blood vessels.[16] Introduction of Id1 into ECs induces EC proliferation and migration.[17,18] Because knockdown of Id1 in ECs treated with BMP perturbs EC activation, Id1 is considered to be essential for BMP-induced EC activation.[18] Loss of Id1 in tumor ECs leads to down-regulation of integrin α6, integrin β4, FGFR1, MMP2, and laminin5.[19] Thus, Id1 positively regulates proangiogenic transcripts even though it cannot bind directly to DNA. Although many bHLH transcription factors have been implicated in EC angiogenic activities, which proteins Id1 regulates remains unclear.

We have reported that Hey1/Herp2/Hesr1, one of the bHLH proteins induced by Notch signaling, antagonizes activated BMP receptor-induced EC migration. This antagonism is caused by the degradation of Id1 interacting with Hey1/Herp2/Hesr1 in ECs. Thus, Id1-induced EC migration is blocked by Hey1/Herp2/Hesr1.[20] However, the mechanism by which Id1 triggers EC angiogenic activation is still poorly understood.

To gain more insight into the molecular mechanisms by which Id1 positively regulates EC activation, we searched for Id1 interaction partners using a yeast 2-hybrid system and identified E2-2. E2-2 (also known as ITF2, TCF4, SEF2, and SEF2-1B) is classified into the E-protein family (or the class A type of bHLH transcription factors), whose expression is virtually ubiquitous. In addition to E2-2, *E2A* and *HEB* also belong to the E-protein family.

Submitted May 20, 2009; accepted February 22, 2010. Prepublished online as *Blood* First Edition paper, March 15, 2010; DOI 10.1182/blood-2009-05-223057.

The online version of this article contains a data supplement.

The publication costs of this article were defrayed in part by page charge payment. Therefore, and solely to indicate this fact, this article is hereby marked "advertisement" in accordance with 18 USC section 1734.

This family of transcription factors recognizes a consensus DNA sequence known as the E-box (CANNTG) in dimer form, whereas monomeric forms have no discernible DNA-binding activity.[21,22] The E-protein family of proteins is known to regulate lymphocyte development,[23] neural differentiation,[24] and myogenesis.[25] Our previous study demonstrated that E2-2 can inhibit the activity of VEGFR2 luciferase reporters in ECs.[26] However, how E2-2 counteracts the activity of the VEGFR2 promoter and whether E2-2 influences the actions of ECs remain veiled. In this study, we explored the role of E2-2 in angiogenesis both in vitro and in vivo. We found that E2-2 represses VEGFR2 promoter activity to inhibit angiogenesis and that E2-2–mediated EC inactivation can be alleviated through interaction with Id1.

Methods

Plasmids and adenoviruses

cDNAs for human and mouse E2-2 as well as mouse LMO2 were cloned by reverse-transcription polymerase chain reaction (RT-PCR). Each cDNA was sequenced before use. E2-2ΔHLH and Id1ΔHLH were generated by Pfx DNA polymerase (Invitrogen) using human E2-2 or mouse Id1 as templates, respectively. Mouse stem cell leukemia hematopoietic transcription factor (SCL) was a kind gift from Dr M. Ema (University of Tsukuba, Japan).[27] cDNAs were inserted into Flag-pcDNA3 or Myc-pcDNA3[28] and subsequently ligated into the pcDEF3 vector.[29] DEF3-Flag-Id1, DEF3-Myc-Id1, and DEF3-Id1 have been previously described.[20] MCKpfos-luc and pGL2b-VEGFR2-luc (−166 bp/267 bp) were generously provided by Drs M. Sigvardsson (Lund University, Sweden) and C. C. W. Hughes (University of California, Irvine), respectively.[26,30,31] VEGFR2-luc mutant constructs were also generated by PCR. After verification of each sequence, reporter constructs were used for each experiment. Adenoviruses expressing Myc-E2-2 were generated using the pAdTrack-CMV vector.[32] After recombination of pAdTrack-CMV-Myc-E2-2 with pAdEasy-1,[32] the resulting plasmid was transfected into 293T cells, and adenoviruses were amplified. Adenoviruses expressing Flag-Id1 have been reported.[20]

Cell culture

COS7 cells and mouse embryonic endothelial cells (MEECs)[17] were maintained in Dulbecco modified Eagle medium (DMEM; Invitrogen) containing 10% fetal calf serum (FCS; Invitrogen), minimum essential medium nonessential amino acids (Invitrogen), and 100 U/mL penicillin/streptomycin (Wako). Calf pulmonary aortic endothelial cells (CPAEs)[33] were cultured in DMEM with 10% FCS, 20mM N-2-hydroxyethylpiperazine-N′-2-ethanesulfonic acid (Wako), and 100 U/mL penicillin/streptomycin. Primary human umbilical vein endothelial cells (HUVECs) were cultured in endothelial basal medium (Lonza Walkersville) supplemented with 2% FCS. MEECs and HUVECs were grown on 0.1% gelatin-coated dishes.

Adenoviral infections

Adenoviruses were incubated in DMEM containing polybrene (Sigma-Aldrich; 80 μg/mL) for 2 hours and added to the dishes. Two hours after infection, cells were washed and allowed to recover 24 hours before the experiments. If necessary, cells were starved by removal from the FCS overnight and then stimulated with 50 ng/mL recombinant human VEGF (Wako).

Immunoprecipitation and Western blotting

To detect interactions among the proteins, plasmids were transfected into COS7 cells (5×10^5 cells/6-cm dish) using FuGENE6 (Roche Diagnostics). Forty hours after transfection, the cells were lysed in 500 μL of TNE buffer (10mM Tris [pH 7.4], 150mM NaCl, 1mM ethylenediamine-*N*′, *N*′, *N*′, *N*′-tetraaccetic acid, 1% NP-40, 1mM phenymethylsulfonyl-l-fluoride, 5 μg/mL leupeptin, 100 U/mL aprotinin, 2mM sodium vanadate, 40mM NaF, and 20mM β-glycerophosphate). Cell lysates were precleared with protein G-Sepharose beads (GE Healthcare) for 30 minutes at 4°C and then incubated with anti-Flag M5 antibody (Sigma-Aldrich) for 2 hours at 4°C. Protein complexes were immunoprecipitated by incubation with protein G-Sepharose beads for 30 minutes at 4°C followed by 3 washes with TNE buffer. Immunoprecipitated proteins and aliquots of total cell lysates were boiled for 5 minutes in sample buffer, separated by sodium dodecyl sulfate-polyacrylamide gel electrophoresis, and transferred to Hybond-C Extra membranes (GE Healthcare). The membranes were probed with anti-Myc 9E10 antibody (Santa Cruz Biotechnology). Primary antibodies were detected using horseradish peroxidase-conjugated goat anti–mouse antibody (GE Healthcare) and chemiluminescent substrate (Thermo Electron). Protein expression in total cell lysates was evaluated by Western blotting using anti-Flag M5 or anti-Myc 9E10 antibody. To detect the endogenous interaction between Id1 and E2-2, either an anti–E2-2 monoclonal antibody (anti-TCF4 M03; Abnova) or an anti-Id1 polyclonal antibody (Santa Cruz Biotechnology) was used.

RNA isolation and RT-PCR

Total RNA was isolated using the RNeasy kit (QIAGEN). Reverse transcription was carried out using a First-Strand cDNA Synthesis Kit (Takara). PCR was performed using Taq polymerase (Invitrogen) as directed by the manufacturer. Primer sets used are shown in supplemental Tables 1 and 2 (available on the *Blood* Web site; see the Supplemental Materials link at the top of the online article).

Transcriptional reporter assay

MEECs were seeded at 5×10^4 cells/well in 12-well plates 1 day before transfection.

Cells were transfected using Lipofectamine (Invitrogen) and Plus Reagent (Invitrogen). After 40 hours of transfection, lysates were prepared and luciferase activity was measured using a luciferase assay system (Promega). Results were corrected by measuring β-galactosidase activity (pCH110; GE Healthcare). Each experiment was carried out in triplicate and repeated at least twice. Values represent the mean plus or minus SD ($n = 3$).

Immunofluorescence

Immunofluorescence assay was performed as previously described.[34] Briefly, MEECs grown on the cover glass were stimulated with 25 ng/mL BMP6 to induce Id1. After treatment, the glasses were washed once with phosphate-buffered saline (PBS), fixed for 10 minutes with 4% paraformaldehyde (PFA; Wako), washed 3 times with PBS, subsequently permeabilized with 0.5% Triton X-100 in PBS for 5 minutes, and washed again 3 times with PBS. Glasses were blocked with 5% normal swine serum (Dako Denmark) in PBS at 37°C for 1 hour and incubated with 5% normal swine serum (in PBS) containing mouse monoclonal anti–E2-2 (anti-TCF4 M03) and rabbit polyclonal Id1 antibodies at 4°C overnight. The glasses were then washed 3 times with PBS, incubated with 5% normal swine serum (in PBS) including both fluorescein isothiocyanate-conjugated goat anti–mouse IgG antibody (diluted 1:250; Invitrogen) and Texas red-conjugated goat anti–rabbit IgG antibody (diluted 1: 250; Invitrogen) at room temperature for 1 hour, and washed 3 times with PBS. To visualize the fluorescence, an immunofluorescence microscope (Axiovert 200M; Carl Zeiss) was used.

Migration assay

Cell migration assays were performed using a Boyden chamber. Costar nucleopore filters (8-μm pore diameter) were coated with 10 μg/mL fibronectin (Sigma-Aldrich) overnight at 4°C. The chambers were washed 3 times with PBS. Adenovirus-infected HUVECs starved for 12 hours without FCS were added to the top of each migration chamber at a density of 1.5×10^4 cells/chamber in 150 μL of endothelial basal medium without FCS. Cells were allowed to migrate to the underside of the chamber in the presence or absence of 50 ng/mL VEGF in the lower chamber. After

6 hours, cells were fixed in 4% PFA and stained with 0.5% crystal violet (dissolved in 25% methanol; Wako). The upper surface was wiped with cotton swabs to remove nonmigrating cells. Cells present on the lower surface were counted. Each experiment was carried out in triplicate and repeated several times. Values represent the mean plus or minus SD (n = 3).

Network formation assay

HUVECs (2×10^4 cells/well in an 8-well Lab-Tek chamber; Thermo Electron) infected with adenoviruses were seeded on growth factor-reduced Matrigel (BD Biosciences). Ninety minutes later, images were captured every 15 minutes for 4 hours using a time-lapse microscope (Axiovert 200M; Carl Zeiss) to monitor cell behavior.

Erk phosphorylation

HUVECs were seeded at 1×10^5 cells/well in 12-well plates. Twenty-four hours after HUVECs were infected with the E2-2–expressing adenoviruses, HUVECs were starved without FCS for 12 hours. Then, HUVECs were stimulated with 50 ng/mL VEGF for the indicated times. Phospho-Erk1/2, Erk2, Myc-E2-2, and β-actin were analyzed by Western blots of total cell lysates using antiphospho-Erk(p44/p42) (Cell Signaling), anti-Erk2 (Santa Cruz Biotechnology), anti-Myc9E10 (Santa Cruz Biotechnology), and anti–β-actin (Sigma-Aldrich) antibodies, respectively.

Cell proliferation

Proliferation was measured by direct counting of cultures in 12-well plates. CPAEs were seeded at 1×10^4 cells/well in 12-well plates 1 day before adenoviral infection. We began counting cells 1 day after adenoviral infection.

Mouse angiogenesis assay

The formation of new vessels in vivo was evaluated by Matrigel plug assay with some modifications to the previously described method.[35] Adenoviruses expressing 1×10^9 pfu of green fluorescent protein (GFP), 1×10^9 pfu of E2-2, and/or 2.5×10^8 pfu of Id1 were mixed in the Matrigel solution at 4°C with 200 ng/mL VEGF-A (Wako), 1 μg/mL bFGF (R&D Systems), and 100 μg/mL heparin (Wako). A total of 500 μL of Matrigel-containing adenoviruses was injected subcutaneously into the abdomen of male ICR mice. The mice were killed 7 days after the injection. The Matrigel plugs with adjacent subcutaneous tissues were recovered by en bloc resection, and images were then taken using a stereomicroscope (Leica). Thereafter, each sample was embedded in the optimal cutting temperature (OCT) compound and quickly frozen in liquid nitrogen to be sectioned at a thickness of 5 μm at −18°C. After being fixed with 4% PFA/PBS, anti–rat monoclonal PECAM-1 antibody (1:200 dilution) was used as a primary antibody. Then, the sections were incubated with Alexa568-conjugated goat anti–rat IgG antibody (1:200 dilution; Invitrogen). Images were taken using a fluorescence microscope (Carl Zeiss). Mice were housed in the animal facilities of Laboratory Animal Resource Center in University of Tsukuba under specific pathogen-free conditions with constant temperature and humidity and fed a standard diet. Treatment of mice was approved by the Animal Care and Use Program at the University of Tsukuba.

Knock-down of E2-2

The pLVTHM lentiviral vector for shRNA was purchased from Addgene. Double-strand DNAs for 5′-cgcgtcccc**AGAGCTGAGTGATTTACT**-GttcaagagaCAGTAAATCACTCAGCTCTttttggaaat/3′-aggggTCTCGACT-CACTAAATGACaagttctctGTCATTTAGTGAGTCGAGAaaaaaccttagc-5′ (shE2-2#1) and 5′-cgcgtcccc**GAAATTAGATGACGACAAG**ttcaagaga-CTTGTCGTCATCTAATTTCttttggaaat-3′/3′-aggggCTTTAATCTACT-GCTGTTCaagttctctGAACAGCAGTAGATTAAAGaaaaaccttagc-5′ (shE2-2#4) were inserted into pLVTHM digested with both MluI and ClaI. Lentiviral vectors expressing shE2-2 were transfected into 293T cells together with psPAX2 and pMD2.G. The lentiviruses were incubated for 2 hours in DMEM containing polybrene (80 μg/mL) and then added to the dishes. Two hours after being infected, the cells were washed and cultured in medium. Infected HUVECs, which became GFP-positive, were isolated by fluorescence-activated cell sorting and used for the experiments.

Results

Identification of Id1-interacting proteins

To obtain insight into how Id1 activates angiogenesis, we isolated proteins that interact with Id1 using a yeast 2-hybrid system. We used Id1 as bait to screen an amplified human aorta cDNA library (with an original complexity of 3.5×10^6 independent cDNA clones). Among the positive clones identified, the cDNA encoding E2-2 was isolated most frequently. We then investigated whether E2-2 interacts with Id1 in mammalian cells. We also tested the interaction of E2-2 with Herp2, LMO2, and SCL, which are known to modulate EC activation.[20,36-38] As shown in Figure 1A, E2-2 interacted with Id1, SCL,[26] and itself, but not with Herp2 or LMO2. In the reciprocal experiment, Id1 bound strongly with E2-2 and marginally with LMO2 and itself (Figure 1B). When the membrane was exposed for a longer time, an interaction between Id1 and Herp2, which we have described previously,[20] was observed (data not shown). These results indicated that the interaction between Id1 and E2-2 is the most prominent of the combinations tested.

To confirm that the interaction between E2-2 and Id1 is physiologically significant, we investigated the interaction between endogenous proteins in MEECs stimulated with BMP6 for 3 hours because Id1 is known to be induced by BMPs.[39] After cell lysis, immunoprecipitation was performed using an anti–E2-2 antibody. Subsequently, immunoprecipitates were blotted with an anti-Id1 antibody. As shown in Figure 1C, endogenous Id1 formed a complex with endogenous E2-2 in cells. Conversely, the specific band corresponding to E2-2 could be detected (arrow) when cell lysates were immunoprecipitated with an anti-Id1 antibody (supplemental Figure 1). The interaction between E2-2 and Id1 led us to investigate whether E2-2 colocalizes with Id1. To show colocalization of E2-2 with Id1 in ECs, subcellular localization was determined with a fluorescence microscopy by staining E2-2 with fluorescein isothiocyanate-conjugated goat anti–mouse IgG and Id1 with Texas Red-conjugated goat anti–rabbit IgG. E2-2 and Id1 colocalized in nucleus (Figure 1D), which is consistent with an interaction between the 2 proteins. In addition, we used the aorta ring assay to visualize the expressions of E2-2 and Id1 with fluorescent imaging. When both E2-2 and Id1 were costained with fluorescence probes, we recognized that both proteins in sprouting ECs could colocalize in the nucleus (data not shown).

HLH domains play an important role in protein-protein interactions. To examine the contribution of HLH domains to the E2-2/Id1 interaction, we made E2-2 and Id1 mutants lacking the respective HLH domains (supplemental Figure 2A). As shown in supplemental Figure 2B and C, E2-2 did not interact with E2-2ΔHLH or Id1ΔHLH. Similarly, Id1 did not interact with E2-2ΔHLH (supplemental Figure 2D). To further confirm that the HLH domain of E2-2 is enough for E2-2 to interact with Id1, we made an expression construct for GFP, which was fused with the HLH domain derived from E2-2 (GFP-HLH). When GFP-HLH was cotransfected with Id1 in COS7 cells, we could observe the interaction between GFP-HLH and Id1 (supplemental Figure 2E). However, its interaction seemed to be weak. Thus, the other domain(s) of E2-2, except for its HLH domain, might contribute to the adequate interaction between E2-2 and Id1. Taken together, these results indicated that E2-2 heterodimerizes with Id1 and

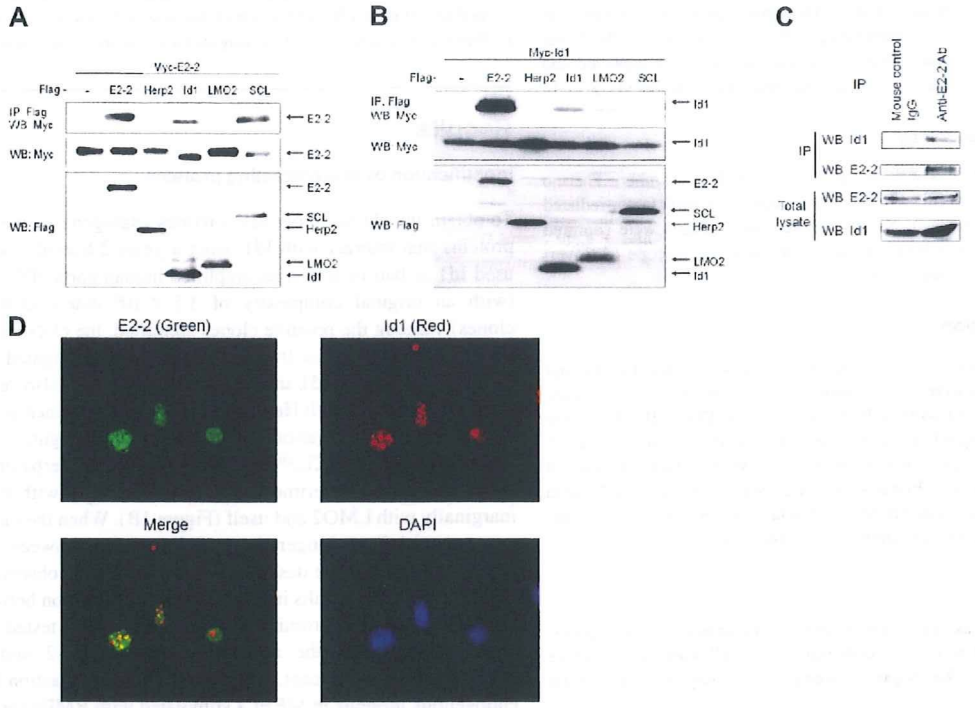

Figure 1. Interaction between E2-2 and Id1. (A) Interaction of Myc-E2-2 with Flag-Id1. Myc-E2-2 was cotransfected with Flag-E2-2, Flag-Herp2, Flag-Id1, Flag-LMO2, or Flag-SCL. Immunoprecipitations were carried out using anti-Flag M5 antibody, and coimmunoprecipitated E2-2 was detected by Western blotting using anti-Myc 9E10 antibody (top panel). The expression of Myc-E2-2 and proteins conjugated with Flag at the N-terminus was evaluated using anti-Myc 9E10 (middle panel) and anti-Flag M5 antibodies (bottom panel), respectively. (B) Interaction of Myc-Id1 with Flag-E2-2. The experiment was performed in a manner similar to that described in panel A. Interaction of Myc-Id1 with Flag-tagged proteins (top panel). Expression of Myc-Id1 and Flag-tagged proteins was checked using anti-Myc 9E10 antibodies (middle panel) and anti-Flag M5 antibodies (bottom panel), respectively. (C) Endogenous interaction between Id1 and E2-2. MEECs were stimulated with BMP6 for 3 hours. Cell lysates were immunoprecipitated with a mouse anti–E2-2 monoclonal antibody, followed by Western blotting with a rabbit anti-Id1 polyclonal antibody (top panel). Expression of E2-2 in immunoprecipitates was checked using an anti–E2-2 monoclonal antibody (second panel). To show expression of E2-2 and Id1 in total lysates, an anti–E2-2 monoclonal antibody (third panel) and an anti-Id1 polyclonal antibody (bottom panel) were used. As a negative control, mouse control IgGs were used for immunoprecipitation. (D) Colocalization of E2-2 with Id1 in MEECs. MEECs were stained with a mouse anti–E2-2 monoclonal antibody (green) or a rabbit anti-Id1 polyclonal antibody (red). Nuclei were visualized using 4′,6-diamidino-2-phenylindole. After samples were mounted with Fluorescent Mounting Medium (Dako Denmark), they were visualized using an immunofluorescence microscope (Axiovert 200M; Carl Zeiss) with a 63×/1.4 oil objective lenses (Carl Zeiss). Images were acquired with AxioCam MRm 60-C1 (Carl Zeiss) and processed with the AxioVision Rel 4.4 (Carl Zeiss) and Adobe Photoshop 7.0.1 software (Adobe).

homodimerizes through its HLH domain. In addition, Id1 requires its HLH domain to associate with E2-2.

Inhibition of E2-2–mediated transcription by Id1

The MCKpfos-luc reporter construct consisting of 4 E-box elements has been used to investigate the function of E-proteins.[26,30] E2-2 enhanced the activity of this reporter in a dose-dependent manner (supplemental Figure 3A), but E2-2ΔHLH was unable to potentiate reporter activity (data not shown). Id proteins have been reported to interact with bHLH transcription factors and prevent them from binding to DNA or forming active heterodimers (or homodimers).[3] Although we did not know whether E2-2 forms a homodimer or a heterodimer with other bHLH proteins in MEECs to activate this reporter, Id1 blocked E2-2–induced reporter activity as anticipated (Figure 2A; supplemental Figure 3B). Consistent with the undetectable interaction between E2-2 and Id1ΔHLH, E2-2–induced reporter activity was not reduced by Id1ΔHLH (Figure 2A).

As we have reported,[26] E2-2 inhibited VEGFR2 reporter activity in MEECs in a dose-dependent manner (supplemental Figure 3C), whereas the introduction of Id1 into MEECs relieved the E2-2–mediated repression (Figure 2B). To show that Id1 indeed hampers E2-2 dimer formation, COS7 cells were cotransfected with Myc-E2-2 and Flag-E2-2 in the absence or presence of Myc-Id1. Immunoprecipitation of COS7 cell extracts revealed that Id1 blocked E2-2 homodimer formation (Figure 2C). We also investigated whether Id1 can disrupt the preexisting E2-2 homodimer. We prepared lysates from cells transfected with either Myc-Id1 or pcDNA3. Subsequently, each lysate was mixed with lysate prepared from cells transfected with both Myc-E2-2 and Flag-E2-2, immunoprecipitated with anti-Flag antibody, and then analyzed by Western blotting with anti-Myc antibody. As seen in Figure 2D, Id1 could efficiently make the preexisting E2-2 homodimer dissociated.

Inhibition of EC activation by E2-2

We speculated that E2-2 would have an opposite effect on EC activation compared with Id1 because Id1 antagonized E2-2–mediated reporter activity. To investigate the effect of E2-2 on network formation, we infected HUVECs with either GFP- or E2-2–expressing adenoviruses before seeding the cells on Matrigel. We then observed the formation of cord-like structures by time-lapse microscopy (Figure 3A). As seen in video (supplemental Figure 4A-B), HUVECs expressing E2-2 did not form cord-like structures as quickly as HUVECs expressing GFP as a control did. We also investigated the effect of E2-2 on cell migration in the presence of VEGF. HUVECs challenged with VEGF after infection with E2-2–expressing adenoviruses exhibited decreased migration

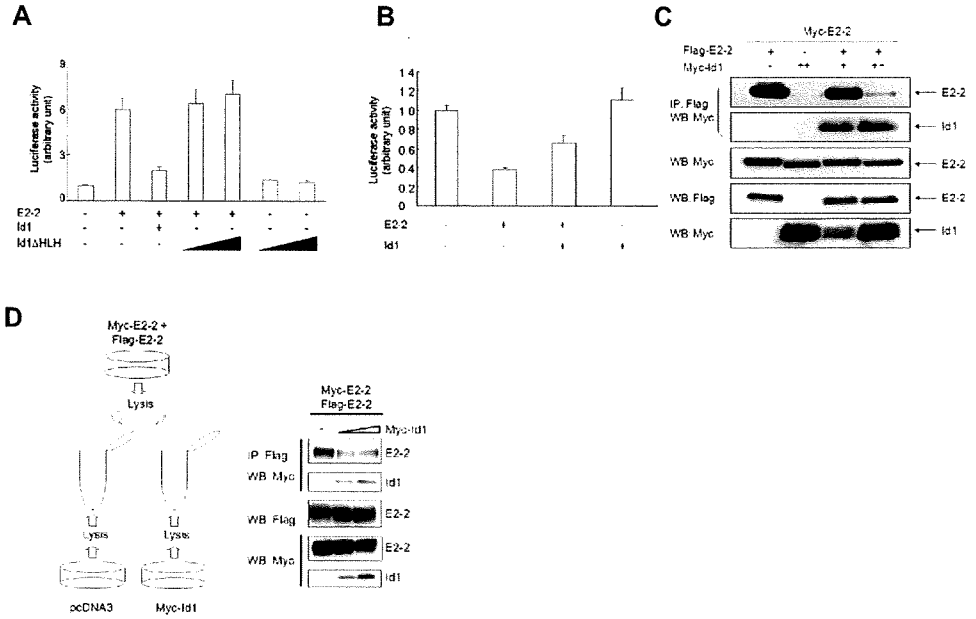

Figure 2. Id1 counteracts E2-2–mediated luciferase activity. (A) Id1ΔHLH does not perturb E2-2–induced MCKpfos-luc activity. MEECs were transfected with MCKpfos-luc, E2-2, and either Id1 or different amounts of Id1ΔHLH. (B) Id1 relieves the inhibition of pGL2b-VEGFR2-luc (−166 bp/267 bp) activity by E2-2. MEECs were transfected with pGL2b-VEGFR2-luc (−166 bp/267 bp), Id1, and E2-2. (C) Id1 disrupts E2-2 homodimer formation. The experiment was performed as described in Figure 1A. E2-2 homodimer formation (top panel) and E2-2/Id1 heterodimer formation (second panel) are shown. Expressions of Myc-E2-2 (third panel) and Myc-Id1 (bottom panel) were evaluated using an anti-Myc 9E10 antibody, and the expression of Flag-E2-2 was shown using an anti-Flag M5 antibody (fourth panel). (D) Id1 disturbs the preexisting E2-2 homodimer formation. Left panel: Illustration of how cell lysates were prepared from each dish in which indicated plasmids were transfected in COS7 cells. Right panel: After each cell lysate was mixed, the experiment was performed as described in Figure 1A. E2-2 homodimer formation (top panel) and E2-2/Id1 heterodimer formation (second panel) are shown. The expression of Flag-E2-2 was shown using an anti-Flag M5 antibody (third panel). Expressions of Myc-E2-2 (fourth panel) and Myc-Id1 (bottom panel) were evaluated using an anti-Myc 9E10 antibody.

compared with cells infected with GFP-expressing adenoviruses (Figure 3B). Because Id1 perturbs the function of E2-2, we examined the possibility that Id1 would relieve the E2-2–mediated repression of the VEGF-induced chemotactic response. Indeed, Id1 marginally rescued the inhibitory effect of E2-2 on VEGF-induced cell migration (Figure 3B). Importantly, VEGF-induced HUVEC migration was also increased when E2-2 levels were decreased via lentiviral expression of human shE2-2s but not in response to control lentiviruses (Figure 3C).

Impairment of in vivo angiogenesis by E2-2

Because E2-2 inhibits EC activation in vitro, we tried to examine whether in vivo angiogenesis would be affected by overexpression of E2-2. To elucidate this possibility, we used the Matrigel plug assay by which the angiogenic (or antiangiogenic) ability of proteins, cytokines, or compounds can be assigned. To overexpress E2-2 and/or Id1, we subcutaneously injected Matrigel mixed with E2-2– and/or Id1-expressing adenoviruses.[35,40] Seven days after implantation of the Matrigel plugs together with adenoviruses expressing E2-2 and/or Id1, the Matrigels were removed. When we investigated whether the protein expression by the method of adenoviral gene transfer was kept for 7 days, GFP-positive cells were detected in the Matrigel plugs (supplemental Figure 5). As seen in Figure 4A, there were fewer blood vessels observed in the Matrigel plugs containing E2-2–expressing adenoviruses than in those containing control adenoviruses. Because Id1 influenced the E2-2–mediated inhibition of EC activation, we mixed the Id1-expressing adenoviruses with E2-2–expressing adenoviruses and injected them into the Matrigel plugs implanted under the skin. As expected, the injection of Id1-expressing adenoviruses restored in vivo angiogenesis suppressed by E2-2. When the cells expressing PECAM-1 were visualized using the frozen sections, there were fewer PECAM-1–positive cells seen in the Matrigel plugs injected with adenoviruses expressing E2-2 than in those injected with control adenoviruses or a combination of Id1-expressing adenoviruses with E2-2–expressing adenoviruses (Figure 4B-C). These results indicated that, in contrast to Id1, E2-2 is an antagonistic molecule for angiogenic reaction.

To investigate the mechanism by which E2-2 inhibits angiogenic reaction both in vitro and in vivo, we examined the expression of several genes known to be implicated in angiogenesis (eg, VEGFR1, VEGFR2, VEGF, PECAM-1, and VE-cadherin). Of the genes examined, VEGFR2 mRNA was considerably reduced in both human and bovine ECs after infection with E2-2–expressing adenoviruses (Figure 4D); the expression of VEGF was marginally decreased by E2-2. VEGFR1, PECAM-1, and VE-cadherin mRNA levels, however, did not change in response to E2-2 overexpression (Figure 4D). Because VEGFR2 mRNA was prominently decreased by E2-2, we were prompted to check its protein expression after the infection of E2-2 to HUVECs. Consistent with the result of VEGFR2 mRNA expression, E2-2 slightly inhibited the expression of VEGFR2 protein, whereas Id1 partially rescued decrease of VEGFR2 protein mediated by E2-2 (supplemental Figure 6B).

VEGF signaling through the activation of the VEGFR2 receptor elicits multiple effects on ECs, such as migration, proliferation, survival, and differentiation.[41] One of the signaling pathways downstream of VEGF/VEGFR2 is the MAP kinase pathway. When HUVECs were stimulated with VEGF, Erk was transiently phosphorylated (Figure 4E). Its phosphorylation peaked at 10 minutes after VEGF stimulation and declined rapidly thereafter. When E2-2 was overexpressed in HUVECs

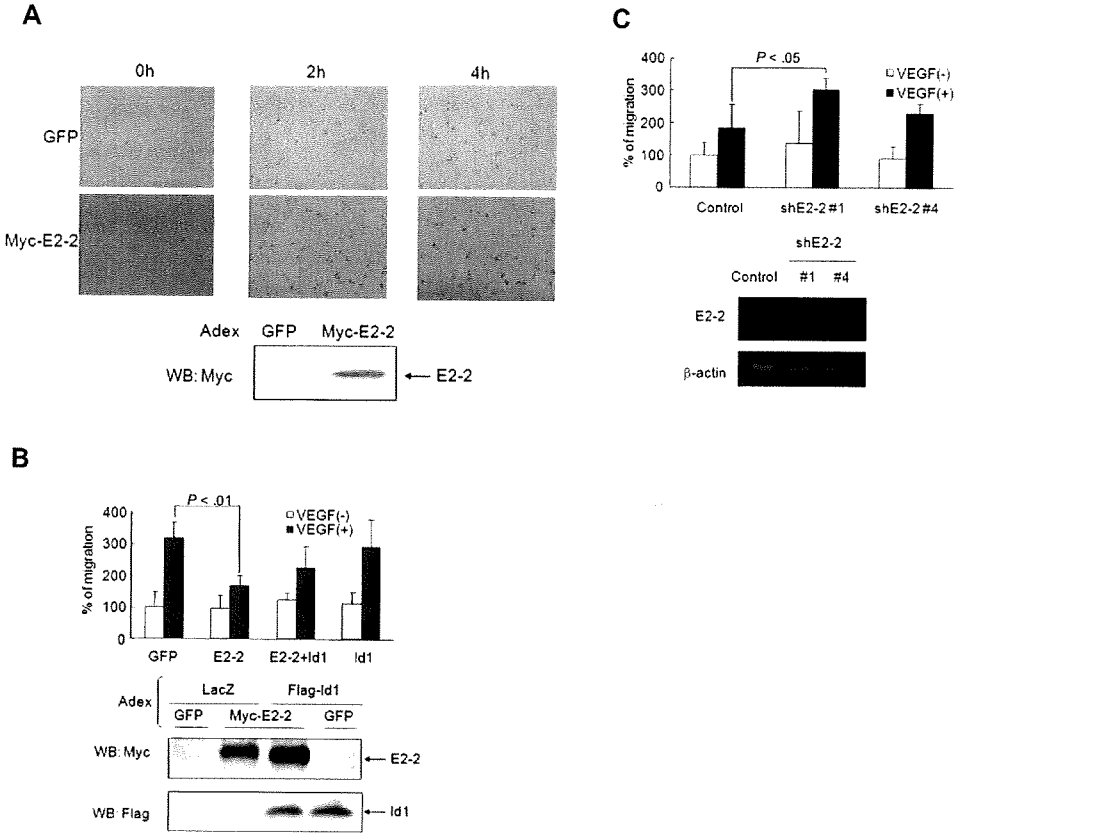

Figure 3. E2-2 blocks EC activation. (A) E2-2 inhibits the formation of cord-like structures on the Matrigel. Forty hours after adenoviral infection, HUVECs were seeded on the Matrigel. Ninety minutes later, images were recorded every 15 minutes by time-lapse microscopy (supplemental Figure 4A-B). The images at 0-, 2-, and 4-hour time points are shown. Bottom panel: Expression of Myc-E2-2. Samples were visualized using a conventional microscope (Axiovert 200M; Carl Zeiss) with a 5×/0.12 dry objective lenses (Carl Zeiss). Images were acquired with AxioCam MRm 60-C1 (Carl Zeiss) and processed with the AxioVision Rel 4.4 (Carl Zeiss) and Adobe Photoshop 7.0.1 software (Adobe). (B) Id1 rescues E2-2–mediated inhibition of cell migration. After adenoviral infection, HUVECs were seeded on the upper membrane of the Boyden chamber. VEGF (50 ng/mL) was added to the lower chamber. After 6 hours, cells were stained with crystal violet, and the number of transmigrated cells was counted. Adenoviruses expressing LacZ or GFP were used as controls. Values represent the mean plus or minus SD (n = 3). Bottom panels: Myc-E2-2 and Flag-Id1 expression levels. Significant difference was calculated by the Student *t* test. (C) shE2-2 enhances VEGF-induced effect on HUVEC migration. Lentiviruses expressing GFP alone, shE2-2#1, or shE2-2#4 were infected in HUVECs. After sorting lentivirus-infected cells using GFP as a marker, sorted HUVECs were used for migration assay as described in panel B. Bottom panels: Expressions of E2-2 and β-actin by RT-PCR. Values represent the mean plus or minus SD (n = 3). Significant difference was calculated by the Student *t* test.

by adenoviral gene transfer, VEGF induced phosphorylation of Erk with similar kinetics to those of HUVECs infected with GFP-expressing adenoviruses; however, the extent of Erk phosphorylation was diminished (Figure 4E-F). Consistent with the inhibition of VEGF-induced Erk phosphorylation by E2-2, CPAEs and HUVECs expressing E2-2 proliferated more slowly than those expressing GFP (Figure 4G; supplemental Figure 6C). Taken together, these observations support the idea that E2-2 has the ability to inhibit EC activation by antagonizing VEGF signaling.

Id1 has been implicated in the regulation of the expression of integrin α6, integrin β4, FGFR1, MMP2, and laminin5; loss of Id1 results in decreased protein levels.[19] Because Id1 antagonizes the function of E2-2, we hypothesized that genes suppressed transcriptionally by the loss of Id1 might be negatively regulated by E2-2. Transcript levels of MMP2 and integrin β4, but not of other genes, in ECs were reduced by overexpression of E2-2 (Figure 4D; and data not shown). Thus, E2-2 may also block EC activation through transcriptional repression of other proangiogenic genes.

Suppression of VEGFR2 promoter by E2-2

Because ectopic E2-2 reduced VEGFR2 mRNA levels in ECs (Figure 4D), we tried to determine which regions of the VEGFR2 promoter could be affected by E2-2. We tested several VEGFR2 promoter constructs truncated downstream of position −166 for E2-2 responsiveness. Basal reporter activity was greatly reduced on removal of the sequence between −80 and −40. However, all of the constructs were strongly inhibited by E2-2 in a dose-dependent manner (Figure 5A). Two typical E-boxes located in the 5′ noncoding region of the VEGFR2 gene were predicted to be involved in the inhibition of VEGFR2 promoter activity by E2-2. To test this hypothesis, we made 7 3′-truncation mutants of the VEGFR2 promoter (Figure 5B). Basal reporter activity gradually decreased as the 5′ noncoding region was truncated. Unexpectedly, E2-2 could still attenuate the luciferase activity even when both E-boxes were deleted. Furthermore, the activity of pGL2b-VEGFR2-luc (−40 bp/5 bp) was also inhibited by E2-2 despite very low basal luciferase activity. GATA-1 and/or GATA-2 are known to positively regulate VEGFR2 promoter activity by binding to the 5′ noncoding region (98-122 bp).[42] However, the basal activity of the reporter lacking the GATA binding site (pGL2b-VEGFR2-luc [-80 bp/93 bp]) remained at 60% of the reporter activity with the binding site included (pGL2b-VEGFR2-luc, −80 bp/159 bp). Thus, it appears that neither GATA sequences nor E-boxes are required for E2-2 to repress the activity of the VEGFR2 promoter.

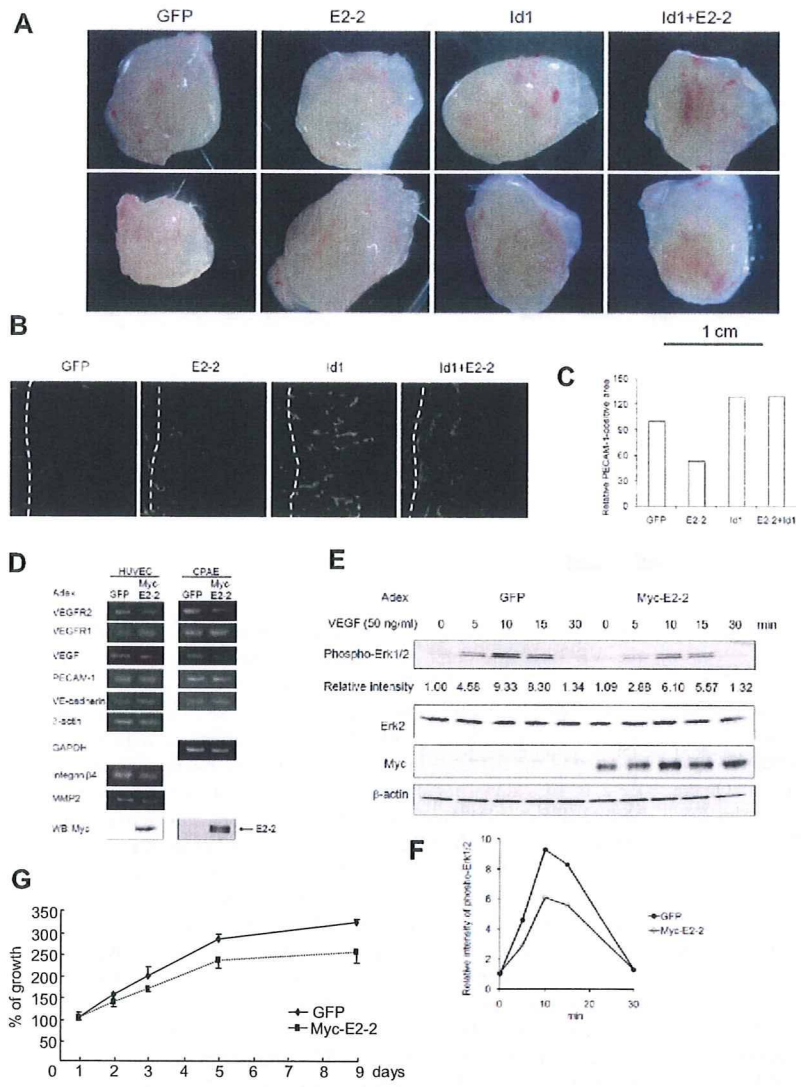

Figure 4. Suppression of angiogenesis by E2-2. (A) Photographs for en bloc resection, including Matrigel plugs with adjacent subcutaneous tissues. Samples were visualized using a stereomicroscope (S8APO; Leica). Images were acquired with EC3 (Leica) and processed with the LAS EZ (Leica) and Adobe Photoshop 7.0.1 software (Adobe). (B) PECAM-1 staining of frozen sections. Matrigels are located to the right side of broken lines, whereas there are mouse subcutaneous tissues to the left side of broken lines. PECAM1-positive areas are shown as white. After samples were mounted with Fluorescent Mounting Medium (Dako Denmark), they were visualized using an immunofluorescence microscope (Axiovert 200M; Carl Zeiss) with a 63 ·/1.4 oil objective lenses (Carl Zeiss). Images were acquired with AxioCam MRm 60-C1 (Carl Zeiss) and processed with the AxioVision Rel 4.4 (Carl Zeiss) and Adobe Photoshop 7.0.1 software (Adobe). (C) Relative PECAM-1-positive area in Matrigel plugs. Five fields were randomly chosen in each condition from panel B, and PECAM-1-positive areas were scored using the imaging software. PECAM-1-positive areas were normalized with the areas of the field. Each relative PECAM-1-positive area was calculated by the comparison of the score in Matrigel plugs, including GFP. (D) Effect of E2-2 on the expression of mRNAs implicated in EC activation. mRNAs involved in EC activation were analyzed by RT-PCR. HUVECs or CPAEs were infected with adenoviruses expressing E2-2 or GFP as a negative control. Gene transcript names are indicated to the left of the figure. mRNAs for β-actin and GAPDH were included as internal controls. The expression of Myc-E2-2 was evaluated in total cell lysates using an anti-Myc 9E10 antibody (bottom panel). Adex indicates adenovirus. To show that EC markers are expressed in CPAEs, RT-PCR was carried out (supplemental Figure 6A). (E) E2-2 inhibits VEGF-induced Erk phosphorylation. Phospho-Erk1/2 (top panel), Erk2 (second panel), Myc-E2-2 (third panel), and β-actin (bottom panel) levels were analyzed by Western blots of total cell lysates. Adenoviruses expressing GFP were used as a negative control. The expression for phosphorylation of Erk1/2 was normalized using the intensity of the band corresponding to Erk2. Each relative intensity was calculated by the comparison of the value for cells infected with GFP-expressing adenoviruses in the absence of VEGF. (F) Graphical presentation for relative intensity of phospho-Erk1/2 levels in panel E: ● represents GFP-expressing adenoviruses; ○, Myc-E2-2–expressing adenovirusues. (G) E2-2 perturbs EC proliferation. Each experiment was performed in triplicate and repeated a few times. Values represent the mean plus or minus SD (n = 3).

We next explored the effect of Id1 on the E2-2–mediated repression of VEGFR2 promoter activity. For this purpose, we used pGL2b-VEGFR2-luc (−80 bp/5 bp) instead of pGL2b-VEGFR2-luc (−40 bp/5 bp) because the basal activity of pGL2b-VEGFR2-luc (−40 bp/5 bp) was quite low. Similar to the effect of Id1 on the pGL2b-VEGFR2-luc (−166 bp/267 bp) reporter (Figure 2B), Id1 relieved the E2-2–mediated repression of pGL2b-VEGFR2-luc (−80 bp/5 bp) activity (Figure 5C), but Id1ΔHLH did not (data not shown). This evidence further convinced us that E2-2 negatively regulates the VEGFR2 promoter. Because the HLH domain of E2-2 is required to activate the MCKpfos-luc reporter (data not shown), we also tested the effect of E2-2ΔHLH on the activity of the VEGFR2 promoter. As expected, E2-2ΔHLH was not capable of inhibiting VEGFR2 promoter activity (data not shown). To test the possibility that E2-2 can bind to the VEGFR2 promoter (from −40 to 5), we performed electrophoresis mobility shift assay using glutathione S-transferase (GST) fusion proteins. GST or GST-Id1 showed no specific binding to the VEGFR2 promoter. However, a specific shifted band appeared when GST-E2-2 was mixed with the probe. Interestingly, the shifted complex decreased when GST-Id1 was added to the mixture containing GST-E2-2 and the probe (supplemental Figure 7A). To further confirm that Id1 promotes the dissociation of E2-2 from the VEGFR2 promoter, we carried out chromatin immunoprecipitation analysis using HUVECs infected with E2-2– and/or Id1-expressing adenoviruses. In the presence of Id1, the VEGFR2 promoter showed decrease in E2-2 binding (supplemental Figure 7B). These results support the data that Id1 rescues E2-2–mediated repression of VEGFR2 promoter activity.

Discussion

It is widely accepted that ubiquitous bHLH proteins, such as E2-2 and E2A, interact with tissue-restricted bHLH proteins to bind consensus E-box sequences and activate transcription of target genes. E-proteins are pivotal in the regulation of cell proliferation and differentiation. For example, E2-2 and its family member E2A play critical roles in B-cell development and perturbed T-cell development.[43-45] In the present study, we found that E2-2 could inhibit angiogenesis in Matrigel plugs implanted under the skin,

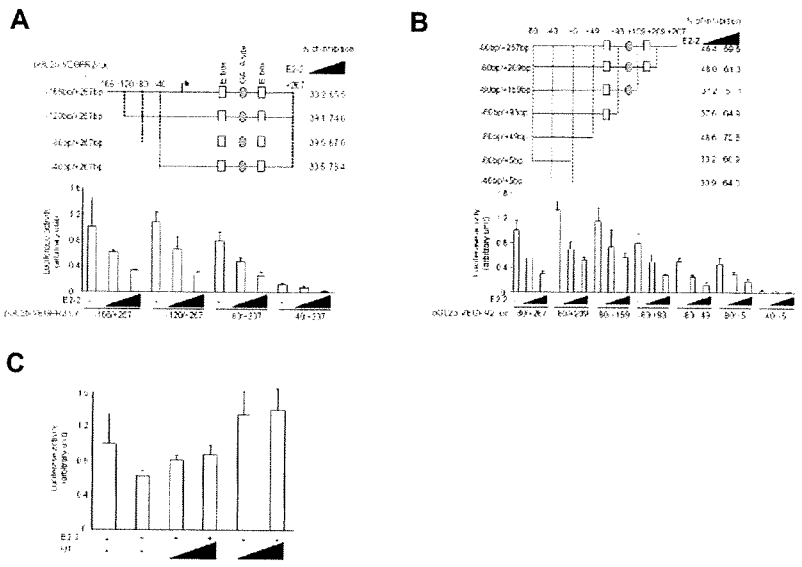

Figure 5. Analysis of the VEGFR2 promoter. (A) Effect of E2-2 on 5′ deletion mutants of the VEGFR2 promoter. MEECs were transfected with 1 of the indicated reporters with different amounts of E2-2. The inhibition percentage of reporter activities by E2-2 is indicated to the right of the top panel. (B) Effect of E2-2 on 3′ deletion mutants of the VEGFR2 promoter. The experiment was carried out as described in panel A. (C) Effect of Id1 on E2-2–mediated suppression of VEGFR2 promoter activity. Different amounts of Id1 (0.1 and 0.5 pg) were transfected together with E2-2. The experiment was carried out as described in panel A.

whereas Id1 overcame E2-2–mediated antagonism of angiogenesis in vivo.

We showed that E2-2 associated with Id1 in MEECs (Figure 1C; supplemental Figure 1A). Consistent with this interaction, Id1 blocked the E2-2–induced activity of the artificial E-box–containing reporter (MCKpfos-luc) in a manner dependent on the HLH domains of Id1 (Figure 2A; supplemental Figure 3B). On the other hand, E2-2 blocked the VEGFR2 reporter activity in ECs independently of typical E-box sequences (Figure 5B).[26] Although E2-2 generally activates the transcription of target genes by forming dimers with other bHLH proteins, a few reports have shown that E2-2 can interfere with transcription.[46,47] In the present study, we clarified that E2-2 negatively regulated the activity of the VEGFR2 promoter, which does not possess typical E-box sequences. However, the VEGFR2 promoter from −40 to 5 contains one imperfect E-box sequence (CANNTC), which has been identified as one of the binding sites of E2-2.[46] It is possible that E2-2 negatively regulates the transcription of the VEGFR2 gene through its binding to the imperfect E-box sequence because GST-E2-2 could make a specific complex with this promoter region. Excepting that possibility, E2-2 might displace TFII-I from the initiator (inr) sequences or interact with TFII-I on inr sequences to prevent TFII-I from activating transcription because TFII-I was recently found to enhance VEGFR2 transcription in an inr-dependent fashion.[48] Further investigation is needed to examine in detail how E2-2 inhibits VEGFR2 promoter activity. In an analogous fashion to E2-2, we found that E2A potentiated and inhibited MCKpfos-luc activity and VEGFR2-luc activity, respectively (supplemental Figure 8A-B), and also interacted with Id1 (supplemental Figure 8C). Furthermore, Id1 perturbed E2A-induced MCKpfos-luc activity (supplemental Figure 8A). These observations provide further evidence that E-protein family members interfere with EC activation. The mechanism by which Id1 potentiates EC activation has not been fully explored. Our study demonstrates one possible mechanism by which Id1 enhances EC activation: by antagonizing the inhibitory function of E2-2 on VEGFR2 promoter activity (supplemental Figure 9).

A number of transcription factors, such as SCL, Ets, Sp1, and NF-κB, have been identified as positive regulators of the VEGFR2 promoter.[49-52] E2-2 may also modulate the activity of these transcription factors, although the sequences between −40 and 5 of the VEGFR2 promoter are critical for the ability of E2-2 to negatively regulate VEGFR2 promoter activity.

The mRNA expressions of integrin β4 and MMP2, both of which are thought to be involved in EC activation, are reduced on ablation of the Id1 gene in cells.[19] As expected, overexpression of E2-2 in ECs down-regulated the transcripts of integrin β4 and MMP2 (Figure 4D). Hey1/Herp2/Hesr1 has been shown to inhibit the activity of both the MMP2 and the VEGFR2 promoters via the inr element.[31] The inhibition of MMP2 transcription by E2-2 might also occur via inr sequences in the MMP2 promoter. Genes other than VEGFR2, integrin β4, and MMP2 that contribute to EC activation may also be negatively regulated by E2-2. We are currently searching for such genes by DNA microarray or chromatin immunoprecipitation (ChIP-on-ChIP) analysis.

The present study demonstrated that E2-2 affects EC activation through suppression of the VEGFR2 transcript as one of its inhibitory actions. The antagonistic actions of E2-2 on EC activation were not so strong that we could exclude other possible explanations for why E2-2 blocks in vivo angiogenesis. Thus, it is possible that E2-2 also possesses the ability to influence vascular smooth muscle cells in addition to ECs to perturb angiogenic reaction in vivo. Therefore, we need to further investigate the action of E2-2 on vascular smooth muscle cells.

The addition of Id1 restored E2-2–mediated inhibition of angiogenesis. E2-2 is ubiquitously expressed, whereas Id1 is induced by a number of proangiogenic factors.[3] The function of Id1 can also be regulated by the subcellular localization during angiogenesis.[53] Thus, the balance between E2-2 and Id1 in the nucleus might determine either the activation or the resolution phase in ECs. It is possible that a compound that enhances the expression of E2-2 in ECs might provide an effective drug to inhibit tumor angiogenesis.

Recently, Deleuze et al reported that E2A (also known as E12/E47) together with SCL and LMO2 could up-regulate VE-cadherin expression to potentiate EC activation.[38] The E2-2–mediated EC suppression observed in our present study conflicts with that report. However, in their report, E2A alone did not enhance VE-cadherin expression, although the knock-down of E2A did inhibit VE-cadherin expression.[38] Furthermore, there is no

evidence that E2A overexpression can activate ECs. We have presented evidence clearly demonstrating that E2-2 overexpression inactivates ECs. In addition, E2A alone, like E2-2, blocked VEGFR2-luc reporter activity (supplemental Figure 8B). It is possible that the bilateral activation of ECs by E-proteins is dependent on the presence of other cofactors, such as SCL and LMO2.

Mice lacking the E2-2 gene are initially viable but die within 1 week of birth. No vascular abnormality in E2-2–deficient embryos is observed.[54] It is possible that related genes (E2A and HEB) might compensate for E2-2 gene deficiency during development. If EC-specific knockout mice bearing triple deletions of the E2-2, E2A, and HEB genes can be established, vascular defect(s) might then be seen.

In conclusion, we discovered a novel mechanism by which E2-2 impairs VEGFR2 transcription in ECs. Id1 can overcome the inhibitory effect of E2-2 on VEGFR2 transcription to potentiate EC activation. The identification of compounds that bolster E2-2 activity in an EC-specific manner may provide an exciting opportunity to modulate tumor angiogenesis for therapeutic intervention.

Acknowledgments

The authors thank Dr M. Ema for mouse SCL cDNA, Dr K. Sampath for BMP-6, and Ms F. Miyamasu for excellent English revision.

This work was supported by Grants-in-aid for Scientific Research (17390073, 20012007, 21590328; M.K., S.I.); a Genome Network Project grant (M.K.) from the Japanese Ministry of Education, Culture, Sports, Science and Technology; a Grant-in-Aid for Fellows from the Japan Society for the Promotion of Science (F.I.); the University of Tsukuba Research Project (M.K.); an AstraZeneca Research Grant 2004 (S.I.); the Kowa Life Science Foundation (S.I.); and the Kato Memorial Bioscience Foundation (S.I.).

Authorship

Contribution: A.T. performed most of the research and analyzed the data; F.I. performed the yeast 2-hybrid experiment and critically reviewed the manuscript; K.N. carried out aorta ring assay, interpreted the data, and critically reviewed the manuscript; T.T. contributed to the network formation assay; S.I. designed most aspects of the research, interpreted the data, and drafted the manuscript; and H. K. and M.K. designed parts of the research, interpreted the data, and critically reviewed the manuscript.

Conflict-of-interest disclosure: The authors declare no competing financial interests.

Correspondence: Susumu Itoh, Department of Biochemistry, Showa Pharmaceutical University, 3-3165, Higashi-Tamagawa Gakuen, Machida, Tokyo 194-8543, Japan; e-mail: sitoh@ac.shoyaku.ac.jp.

References

1. Carmeliet P. Angiogenesis in life, disease and medicine. *Nature.* 2005;438(7070):932-936.
2. Adams RH, Alitalo K. Molecular regulation of angiogenesis and lymphangiogenesis. *Nat Rev Mol Cell. Biol.* 2007;8(6):464-478.
3. Perk J, Iavarone A, Benezra R. Id family of helix-loop-helix proteins in cancer. *Nat Rev Cancer.* 2005;5(8):603-614.
4. Lasorella A, Noseda M, Beyna M, Yokota Y, Iavarone A. Id2 is a retinoblastoma protein target and mediates signalling by Myc oncoproteins. *Nature.* 2000;407(6804):592-598.
5. Ohtani N, Zebedee Z, Huot TJ, et al. Opposing effects of Ets and Id proteins on p16INK4a expression during cellular senescence. *Nature.* 2001;409(6823):1067-1070.
6. Benezra R, Davis RL, Lockshon D, Turner DL, Weintraub H. The protein Id: a negative regulator of helix-loop-helix DNA binding proteins. *Cell.* 1990;61(1):49-59.
7. Jen Y, Weintraub H, Benezra R. Overexpression of Id protein inhibits the muscle differentiation program: in vivo association of Id with E2A proteins. *Genes Dev.* 1992;6(8):1466-1479.
8. Langlands K, Yin X, Anand G, Prochownik EV. Differential interactions of Id proteins with basic-helix-loop-helix transcription factors. *J Biol Chem.* 1997;272(32):19785-19793.
9. Ying QL, Nichols J, Chambers I, Smith A. BMP induction of Id proteins suppresses differentiation and sustains embryonic stem cell self-renewal in collaboration with STAT3. *Cell.* 2003;115(3):281-292.
10. Hollnagel A, Oehlmann V, Heymer J, Ruther U, Nordheim A. *Id* genes are direct targets of bone morphogenetic protein induction in embryonic stem cells. *J Biol Chem.* 1999;274(28):19838-19845.
11. Nakashima K, Takizawa T, Ochiai W, et al. BMP2-mediated alteration in the developmental pathway of fetal mouse brain cells from neurogenesis to astrocytogenesis. *Proc Natl Acad Sci U S A.* 2001;98(10):5868-5873.
12. Katagiri T, Yamaguchi A, Komaki M, et al. Bone morphogenetic protein-2 converts the differentiation pathway of C2C12 myoblasts into the osteoblast lineage. *J Cell Biol.* 1994;127(6):1755-1766.
13. Lopez-Rovira T, Chalaux E, Massagué J, Rosa JL, Ventura F. Direct binding of Smad1 and Smad4 to two distinct motifs mediates bone morphogenetic protein-specific transcriptional activation of *Id1* gene. *J Biol Chem.* 2002;277(5):3176-3185.
14. Ogata T, Wozney JM, Benezra R, Noda M. Bone morphogenetic protein 2 transiently enhances expression of a gene, Id (inhibitor of differentiation), encoding a helix-loop-helix molecule in osteoblast-like cells. *Proc Natl Acad Sci U S A.* 1993;90(19):9219-9222.
15. Kowanetz M, Valcourt U, Bergström R, Heldin C-H, Moustakas A. Id2 and Id3 define the potency of cell proliferation and differentiation responses to transforming growth factor β and bone morphogenetic protein. *Mol Cell Biol.* 2004; 24(10):4241-4254.
16. Lyden D, Young AZ, Zagzag D, et al. Id1 and Id3 are required for neurogenesis, angiogenesis and vascularization of tumour xenografts. *Nature.* 1999;401(6754):670-677.
17. Goumans M-J, Valdimarsdottir G, Itoh S, Rosendahl A, Sideras P, ten Dijke P. Balancing the activation state of the endothelium via two distinct TGFβ type I receptors. *EMBO J.* 2002; 21(7):1743-1753.
18. Valdimarsdottir G, Goumans M-J, Rosendahl A, et al. Stimulation of Id1 expression by bone morphogenetic protein is sufficient and necessary for bone morphogenetic protein-induced activation of endothelial cells. *Circulation.* 2002;106(17):2263-2270.
19. Ruzinova MB, Schoer RA, Gerald W, et al. Effect of angiogenesis inhibition by *Id* loss and the contribution of bone-marrow-derived endothelial cells in spontaneous murine tumors. *Cancer Cell.* 2003;4(4):277-289.
20. Itoh F, Itoh S, Goumans M-J, et al. Synergy and antagonism between Notch and BMP receptor signaling pathways in endothelial cells. *EMBO J.* 2004;23(3):541-551.
21. Lazorchak A, Jones ME, Zhuang Y. New insights into E-protein function in lymphocyte development. *Trends Immunol.* 2005;26(6):334-338.
22. Sun XH. Multitasking of helix-loop-helix proteins in lymphopoiesis. *Adv Immunol.* 2004;84:43-77.
23. Murre C. Helix-loop-helix proteins and lymphocyte development. *Nat Immunol.* 2005;6(11): 1079-1086.
24. Einarson MB, Chao MV. Regulation of Id1 and its association with basic helix-loop-helix proteins during nerve growth factor-induced differentiation of PC12 cells. *Mol Cell Biol.* 1995;15(8):4175-4183.
25. Puri PL, Sartorelli V. Regulation of muscle regulatory factors by DNA-binding, interacting proteins, and post-transcriptional modifications. *J Cell Physiol.* 2000;185(2):155-173.
26. Tanaka A, Itoh F, Itoh S, Kato M. TAL1/SCL relieves the E2-2-mediated repression of VEGFR2 promoter activity. *J Biochem.* 2009;145(2):129-135.
27. Ema M, Faloon P, Zhang WJ, et al. Combinatorial effects of *Flk1* and *Tal1* on vascular and hematopoietic development in the mouse. *Genes Dev.* 2003;17(3):380-393.
28. Kawabata M, Inoue H, Hanyu A, Imamura T, Miyazono K. Smad proteins exist as monomers *in vivo* and undergo homo- and hetero-oligomerization upon activation by serine/threonine kinase receptors. *EMBO J.* 1998;17(14):4056-4065.
29. Goldman LA, Cutrone EC, Kotenko SV, Krause CD, Langer JA. Modifications of vectors pEF-BOS, pcDNA1 and pcDNA3 result in improved convenience and expression. *Biotechniques.* 1996;21(6):1013-1015.
30. Sigvardsson M. Overlapping expression of early B-cell factor and basic helix-loop-helix proteins as a mechanism to dictate B-lineage-specific activity of the λ5 promoter. *Mol Cell Biol.* 2000;20(10): 3640-3654.

31. Holderfield MT, Henderson Anderson AM, Kokubo H, et al. HESR1/CHF2 suppresses VEGFR2 transcription independent of binding to E-boxes. *Biochem Biophys Res Commun.* 2006; 346(3):637-648.
32. He T-C, Zhou S, da Costa LT, Yu J, Kinzler KW, Vogelstein B. A simplified system for generating recombinant adenoviruses. *Proc Natl Acad Sci U S A.* 1998;95(5):2509-2514.
33. Takezawa T, Takenouchi T, Imai K, Takahashi T, Hashizume K. Cell culture on thin tissue sections commonly prepared for histopathology. *FASEB J.* 2002;16(13):1847-1849.
34. Itoh F, AsaoH, Sugamura K, Heldin C-H, ten Dijke P, Itoh S. Promoting bone morphogenetic protein signaling through negative regulation of inhibitory Smads. *EMBO J.* 2001;20(15): 4132-4142.
35. Kano MR, Morishita Y, Iwata C, et al. VEGF-A and FGF-2 synergistically promote neoangiogenesis through enhancement of endogenous PDGF-B-PDGFRβ signaling. *J Cell Sci.* 2005; 118(16):3759-3768.
36. Yamada Y, Pannell R, Forster A, Rabbitts TH. The oncogenic LIM-only transcription factor Lmo2 regulates angiogenesis but not vasculogenesis in mice. *Proc Natl Acad Sci U S A.* 2000;97(1):320-324.
37. Lazrak M, Deleuze V, Noel D, et al. The bHLH TAL-1/SCL regulates endothelial cell migration and morphogenesis. *J Cell Sci.* 2004;117(7): 1161-1171.
38. Deleuze V, Chalhoub E, El-Hajj R, et al. TAL-1/SCL and its partners E47 and LMO2 up-regulate VE-cadherin expression in endothelial cells. *Mol Cell Biol.* 2007;27(7):2687-2697.
39. Korchynskyi O, ten Dijke P. Identification and functional characterization of distinct critically important bone morphogenetic protein-specific response elements in the Id1 promoter. *J Biol Chem.* 2002;277(7):4883-4891.
40. Skurk C, Maatz H, Rocnik E, Bialik A, Force T, Walsh K. Glycogen-synthase kinase3β/β-catenin axis promotes angiogenesis through activation of vascular endothelial growth factor signaling in endothelial cells. *Cir Res.* 2005;96(3):308-318.
41. Olsson AK, Dimberg A, Kreuger J, Claesson-Welsh L. VEGF receptor signaling: in control of vascular function. *Nat Rev Mol Cell Biol.* 2006;7(5):359-371.
42. Minami T, Rosenberg RD, Aird WC. Transforming growth factor-β_1-mediated inhibition of the *flk-1/KDR* gene is mediated by a 5′-untranslated region palindromic GATA site. *J Biol Chem.* 2001; 276(7):5395-5402.
43. Zhuang Y, Soriano P, Weintraub H. The helix-loop-helix gene E2A is required for B cell formation. *Cell.* 1994;79(5):875-884.
44. Bain G, Maandag EC, Izon DJ, et al. E2A proteins are required for proper B cell development and initiation of immunoglobulin gene rearrangements. *Cell.* 1994;79(5):885-892.
45. Bain G, Quong MW, Soloff RS, Hedrick SM, Murre C. Thymocyte maturation is regulated by the activity of the helix-loop-helix protein, E47. *J Exp Med.* 1999;190(11):1605-1616.
46. Liu Y, Ray SK, Yang X-Q, Luntz-Leybman V, Chiu I-M. A splice variant of E2-2 basic helix-loop-helix protein represses the brain-specific fibroblast growth factor 1 promoter through the binding to an imperfect E-box. *J Biol Chem.* 1998;273(30): 19269-19276.
47. Markus M, Du Z, Benezra R. Enhancer-specific modulation of E protein activity. *J Biol Chem.* 2002;277(8):6469-6477.
48. Jackson TA, Taylor HE, Sharma D, Desiderio S, Danoff SK. Vascular endothelial growth factor receptor-2: counter-regulation by the transcription factors, TFII-I and TFII-IRD1. *J Biol Chem.* 2005; 280(33):29856-29863.
49. Kappel A, Schlaeger TM, Flamme I, Orkin SH, Risau W, Breier G. Role of SCL/Tal-1, GATA, and Ets transcription factor binding sites for the regulation of *Flk-1* expression during murine vascular development. *Blood.* 2000;96(9):3078-3085.
50. Patterson C, Perrella MA, Hsieh CM, Yoshizumi M, Lee ME, Haber E. Cloning and functional analysis of the promoter for KDR/flk-1, a receptor for vascular endothelial growth factor. *J Biol Chem.* 1995;270(39):23111-23118.
51. Hata Y, Duh E, Zhang K, Robinson GS, Aiello LP. Transcription factors Sp1 and Sp3 alter vascular endothelial growth factor receptor expression through a novel recognition sequence. *J Biol Chem.* 1998;273(30):19294-19303.
52. Illi B, Puri P, Morgante L, Capogrossi MC, Gaetano C. Nuclear factor-κB and cAMP response element binding protein mediate opposite transcriptional effects on the Flk-1/KDR gene promoter. *Circ Res.* 2000;86(12):E110-E117.
53. Nishiyama K, Takaji K, Uchijima Y et al. Protein kinase A-regulated nucleocytoplasmic shuttling of Id1 during angiogenesis. *J Biol Chem.* 2007; 282(23):17200-17209.
54. Zhuang Y, Cheng P, Weintraub H. B-lymphocyte development is regulated by the combined dosage of three basic helix-loop-helix genes, *E2A, E2-2* and *HEB. Mol Cell Biol.* 1996;16(6):2898-2905.

Biosci. Biotechnol. Biochem., **74** (4), 759–765, 2010

Effects of Topical Application of α-D-Glucosylglycerol on Dermal Levels of Insulin-Like Growth Factor-I in Mice and on Facial Skin Elasticity in Humans

Naoaki HARADA,[1] Juan ZHAO,[1] Hiroki KURIHARA,[2] Naomi NAKAGATA,[3] and Kenji OKAJIMA[1,†]

[1]*Department of Translational Medical Science Research, Nagoya City University Graduate School of Medical Sciences, Nagoya 467-8601, Japan*
[2]*Department of Physiological Chemistry and Metabolism, University of Tokyo Graduate School of Medicine, Tokyo 113-0033, Japan*
[3]*Division of Reproductive Engineering, Center for Animal Resources and Development, Kumamoto University, Kumamoto 860-0811, Japan*

Received October 29, 2009; Accepted January 14, 2010; Online Publication, April 7, 2010
[doi:10.1271/bbb.90797]

Sensory neurons release calcitonin-gene related peptide (CGRP) on stimulation. We have reported that topical application of capsaicin increases facial skin elasticity by increasing the production of dermal insulin-like growth factor-I (IGF-I) through stimulation of sensory neurons in mice and humans. In this study, we examined whether topical application of α-D-glucosylglycerol (GG), a compound found in Japanese traditional brewed foods such as sake (Japanese rice wine), increases the dermal production of IGF-I in mice and increases the facial skin elasticity in females. GG increased CGRP release and cAMP levels in dorsal root ganglion (DRG) neurons isolated from wild-type mice. Pretreatment with capsazepine, an inhibitor of vanilloid receptor-1 activation, and with KT5720, an inhibitor of protein kinase A, reversed GG-induced increases in CGRP release from DRG neurons. Topical application of GG increased dermal levels of IGF-I, IGF-I mRNA, and collagen in wild-type mice, but not in CGRP-knockout mice. Topical application of GG increased cheek-skin elasticity in 13 female volunteers. These observations strongly suggest that GG increases the production of IGF-I in the skin through sensory neuron stimulation, thereby increasing skin elasticity.

Key words: α-D-glucosylglycerol; calcitonin gene-related peptide; insulin-like growth factor-I; sensory neurons; skin elasticity

Insulin-like growth factor-I (IGF-I) is a basic peptide of 70 amino acids with an almost ubiquitous distribution in various tissues and cells, mediating the growth-promoting actions of growth hormone (GH) and playing important roles in postnatal and adolescent growth.[1)]

Since IGF-I has been found to play an important role in the maintenance of normal skin morphology[2)] and to increase collagen synthesis by fibroblasts *in vitro*,[3)] the detrimental skin morphological changes observed in patients with Laron syndrome might be attributable to reduced IGF-I production.

Capsaicin-sensitive sensory neurons are nociceptive neurons found in many tissues within the lining epithelia and around blood vessels.[4)] These sensory neurons release calcitonin-gene related peptide (CGRP) upon activation of vanilloid receptor-1 (VR-1) by a wide variety of noxious physical and chemical stimuli,[5)] thereby showing sensory-efferent functions. CGRP, a 37-amino acid neuropeptide, is produced in dorsal root ganglion (DRG) neurons by tissue-specific alternative processing of the calcitonin gene.[6)] We have reported that sensory neuron stimulation increases IGF-I production in mice.[7)] Furthermore, we recently found that topical application of capsaicin increases dermal levels of IGF-I, thereby increasing skin elasticity in humans.[8)] In addition, sensory neuron stimulation leading to increased IGF-I production promotes hair growth in mice and humans.[9)]

Sake is a traditional brewed alcoholic beverage in Japan, and is also known as Japanese rice wine. Japanese people have experienced that ingestion of sake has positive effects on the skin condition, and women living in the northern region of Japan, where high amounts of sake are consumed, have a better complexion than those living in other areas of Japan.[10)] These observations suggest that sake might have beneficial effects on the maintenance of skin integrity. Consistently with this notion, topical application and oral ingestion of sake concentrate protected the skin from ultraviolet B-induced epidermal barrier disruption in mice,[11,12)] but the detailed mechanisms underlying these beneficial effects of sake on the skin are not fully understood.

α-D-Glucosylglycerol (GG) is a compound contained at a level of about 0.5% in sake.[13)] GG is formed by transglucosylation to glycerol, which is produced by yeast using α-glucosidase derived from koji (microbes similar to those used in the production of blue cheese) in the sake mash.[13)] GG is thought to function as an intracellular osmoregulator, thereby contributing to the survival of yeast during fermentation.[14)]

† To whom correspondence should be addressed. Tel: +81-52-853-8196; Fax: +81-52-842-3460; E-mail: whynot@med.nagoya-cu.ac.jp
Abbreviations: CGRP, calcitonin gene-related peptide; CPZ, capsazepine; DRG, dorsal root ganglion; GG, α-D-glucosylglycerol; GH, growth hormone; IGF, insulin-like growth factor-I; PKA, protein kinase A; VR-1, vanilloid receptor-1; WT, wild-type

Based on these observations, we hypothesized that GG increases dermal IGF-I production by stimulating sensory neurons, thereby contributing to the maintenance of skin integrity.

In the present study, we examined the effects of GG on CGRP release from DRG neurons isolated from wild-type (WT) mice and, on dermal production of IGF-I in WT and congenital CGRP-knockout (CGRP−/−) mice. Furthermore, we analyzed the effects of topical application of GG on cheek skin elasticity in human female volunteers.

Methods

Reagents. GG is kindly provided by Tatsuuma-Honke Brewing Co., Ltd. (Nishinomiya, Japan). Capsazepine (CPZ), an inhibitor of VR-1 activation,[15] was purchased from Sigma Chemical Co. (St. Louis, MO). KT5720, an inhibitor of protein kinase A (PKA), was purchased from Alexis (Basel, Switzerland). All other reagents were of analytical grade.

Animals. Male C57BL/6 mice (6–8 weeks old; Nihon SLC, Hamamatsu, Japan) were used in this study. The care and handling of the animals was in accordance with the National Institute of Health guidelines. All experimental procedures described below were approved by the Nagoya City University Animal Care Committee.

Generation of αCGRP-knockout mice. The generation of αCGRP-knockout mice was described previously.[16] The mouse CT/αCGRP genomic DNA was cloned from a BALB/c mouse genomic library in EMBL3 using synthetic oligonucleotide probes derived from the mouse CT/αCGRP cDNA sequence. A 7.0-kb fragment containing exons 3 to 5 of the mouse CT/αCGRP gene was subcloned into pBluescript (Stratagene, La Jolla, CA). A targeting vector was constructed by replacing the 1.6-kb XbaI-XbaI fragment encompassing exon 5, which is specific for αCGRP, with the neomycin resistance gene and the flanking thymidine kinase gene. This plasmid was linearized with NotI and introduced into 129/Sv-derived SM-1 ES cells by electroporation, after which the cells were selected in medium containing G418 (300 μg/ml) and ganciclovir (2 μmol/l). Homologous recombinants were identified by PCR and Southern blot analysis. Targeted ES cell clones were injected into C57BL/6 mouse blastocysts to generate chimeric mice. Male chimeras were then crossbred with C57BL/6 females and germline transmission was achieved. Littermates obtained by breeding heterozygotes with the genetic background of the 129/SvXC57BL/6 hybrid were used in phenotypic analysis. Only males were used in this study.

Genotype determination of CGRP-knockout pups. Genomic DNA was extracted from tails of mice as previously described[16] and was used for PCR analysis. PCR was performed using the external primers of the replaced gene fragment. The wild-type allele and the mutant allele gave different band sizes. Primer sequences and PCR conditions have been described.[16]

In vitro *experiments.* Isolation and culture of dorsal root ganglion neurons (DRG) and measurement of CGRP release and intracellular cAMP levels.

DRG isolated from the lumbar, cervical, and thoracic regions were dissected from mice, as described previously.[17] After 5 d in culture, the medium was aspirated gently and washed with serum-free Ham's F-12 medium. The cells were incubated with GG (1, 10, and 100 μM) for 30 min in Ham's F-12 medium containing 1% supplemented calf serum without nerve growth factor. After incubation, the supernatants were sampled and stored −20 °C for CGRP measurement. To determine whether GG increase CGRP release from DRG *via* VR-1 activation, we examined the effects of CPZ, an inhibitor of VR-1 activation,[15] on GG-induced CGRP release from DRG. CGRP levels were determined using a commercial mouse CGRP enzyme immunometric assay kit (SPI-Bio, Massy Cedex, France).

Recent studies indicate that cAMP plays a critical role in CGRP release from sensory neurons by phosphorylating VR-1 through activation of PKA,[18] and that cAMP-dependent PKA activation is critically involved in CGRP production in DRG neurons.[19] Hence we measured intracellular cAMP levels in DRG neurons. We examined the effect of KT5720 on CGRP release from DRG neurons at a concentration of 10 μM, as described previously.[17] After collection of supernatants, plates were placed on ice, media were removed, and cells were washed in ice-cold PBS. Thereafter, ice-cold 65% ethanol were added to each well. The ethanol were collected and dried under nitrogen gas. Intracellular levels of cAMP were determined with an enzyme immunoassay kit (GE Healthcare, Buckinghamshire, UK) according to the manufacturer's instructions.

In vivo *experiments.* Effects of a single topical application of GG solution on dermal IGF-I levels in wild-type (WT) and CGRP-knockout mice.

Topical application of GG solution. Mice were anesthetized with i.p. injections of ketamine (100 mg/kg) and xylazine (10 mg/kg). A GG was dissolved in normal saline. GG solution (100 μl) was applied to the shaved backs of the mice (4 cm^2), as described previously.[8] The skin was removed 30 min after topical application of GG solution or saline and then immediately immersed into liquid nitrogen.

Determination of dermal IGF-I level. Dermal levels of IGF-I were determined in the animals by a modification of methods described previously.[20] The skin was minced and homogenized in a polytron type homogenizer (2 times for 15 s) using 2 ml of 1 N acetic acid according to the manufacturer's instructions. The homogenates were then centrifuged at 3,000 × *g* for 10 min. The supernatants were kept in a deep freezer at −80 °C. The concentration of IGF-I was assayed using a specific enzyme immunoassay kit (Diagnostic Systems Laboratories, Webster, TX).

Determination of dermal CGRP levels. The dermal levels of CGRP were determined in animals by a modification of methods described previously.[21] The skin was minced and homogenized in a polytron type homogenizer (2 times for 15 s) using 2 ml of 2 N acetic acid. The homogenates were bathed in 90 °C water for 20 min and then centrifuged at 4,500 × *g* for 10 min. CGRP was extracted from the supernatant using reverse-phage C18 columns (Amersham, Little Chalfont, UK). The columns were prepared by washing with 5 ml of methanol onto the column, followed by a wash with 20 ml of 0.1% trifluoroacetic acid, and the solvent was evaporated under a stream of nitrogen gas. The concentration of CGRP was assayed using a specific enzyme immunoassay kit (SPI-Bio, Massy Cedex, France).

Quantitative mRNA analysis. Quantitative mRNA analysis was performed as previously described.[22] The tissue was weighed and immersed in liquid nitrogen. Total RNA was extracted from the hippocampus with TRIZOL Reagent (Invitrogen, Carlsbad, CA) according to the manufacturer's instructions. The RNA extracted was used as a template for cDNA reverse transcription. Sample cDNAs were amplified in Model 7700 Sequence detector (Applied Biosystems, Perkin Elmer Japan, Chiba, Japan) with primers, dual-labeled fluogenic probes, and a Taqman PCR Reagent Kit (Applied Biosystems, Branchburgh, NJ). The thermal cycler conditions were 10 min at 95 °C for deactivation and then 40 cycles for 15 s at 95 °C for denaturation and 1 min at 60 °C for bath annealing and extension. Known concentrations of serially diluted IGF-I and β-actin cDNA generated by PCR were used as standards for quantitation of the sample cDNA. The copy numbers of cDNA for IGF-I were standardized to those for β-actin from the same sample in the WT and CGRP−/− mice. The mean value for the WT mice 30 min after topical application of saline was determined to be 1.0.

Measurements of total collagen levels in the skin. The relative content of total collagen was measured spectrophotometrically by a method previously described.[23,24] In this experiment, a GG solution (100 μl) was applied to the shaved backs of mice (4 cm^2) for 14 d. The skin was removed 14 d after topical application of the GG solution and then immersed in 4% paraformaldehyde. Paraffin-embedded tissue was cut into 15-μm sections, and three sections were deparaffinized in xylol, xylol-ethanol (1:1, vol/vol), ethanol-water (1:1, vol/vol), and

water. The sections were then placed in small test tubes (10 × 75 mm) and covered with 0.2 ml of a saturated solution of picric acid in distilled water containing 0.1% fast green FCF and 0.1% Sirius red F3BA. The tubes were covered with aluminum foil and incubated at room temperature for 30 min in a rotary shaker. The fluid was carefully withdrawn, and the sections were repeatedly rinsed with distilled water until the rinse fluid was colorless. One ml of 0.1 N NaOH in absolute methanol (1:1, vol/vol) was then added, and each tube was gently mixed until all color was eluted from the specimen. The eluted color was read in a spectrophotometer at 540 and 605 nm (corresponding to the maximum absorbances of Sirius red and fast green respectively). The corrected absorbance at 540 nm (corrected for the contribution of fast green to the absorbance at 540 nm) was then calculated by subtracting from the absorbance at 540 nm the value corresponding to 29.1% of the optical density at 650 nm. The absorbances at 540 and 605 nm were then divided by their respective color equivalents (2.08 and 38.4) to obtain the amounts of collagen and noncollagen protein in the specimen. An estimate of collagen content was calculated by the percentage of total protein.

Human experiments. Topical application of 0.01% GG in healthy female human volunteers.

The protocol was approved by the Ethics Study Board of Sugikami Hospital (Kumamoto Prefecture, Japan), where the study was done. The study design was a double-blinded and placebo-controlled trial. Informed consent was obtained from 23 healthy human female volunteers (aged 36.0 ± 9.7 years). Topical application of 0.01% GG or vehicle (saline) was done once a day (at night between 10 PM and 11 PM after washing of faces) for 14 d. We randomly assigned the 23 volunteers to two groups: 13 received 0.01% GG and the remaining 10 received vehicle.

Assessment of skin elasticity after topical application of GG in human subjects. Before and after topical application of 0.01% GG or vehicle to the 23 healthy female human volunteers for 14 d, we measured cheek elasticity with a Cutometer MPA580 (Integral, Tokyo), as described previously.[25] In this system, skin elasticity is defined as A (maximal deformation) − B (basal level after removal of vacuum).

Statistical analysis. Data were expressed as mean ± SD. The results were compared by ANOVA followed by Scheffé's *post hoc* test. To determine the difference between the values for skin elasticity obtained in the same subject before and after topical application of 0.01% GG, the statistical significance of the data was calculated by paired *t*-test. A level of $p \leq 0.05$ was considered statistically significant.

Results

Effects of GG on CGRP release and cAMP levels in DRG neurons isolated from WT mice, in vitro

To determine whether GG increases CGRP release from sensory neurons, we examined the effects of GG on the release of CGRP from DRG neurons isolated from WT mice. GG at concentrations higher than 1 μM enhanced the release of CGRP from DRG neurons (Fig. 1A). Cyclic AMP has been found to sensitize sensory neurons through PKA-dependent phosphorylation of VR-1.[18,19,26] To elucidate the mechanism by which GG stimulates sensory neurons, we examined the effects of GG on cAMP levels in DRG neurons isolated from WT mice. As shown in Fig. 1B, GG at concentrations higher than 1 μM increased cellular cAMP levels.

Effects of CPZ, an inhibitor of VR-1 activation, and KT5720, an inhibitor of PKA, on GG-induced CGRP release from DRG neurons isolated from WT mice

Pretreatment with CPZ, an inhibitor of VR-1 activation, did not have any effect on the baseline release of CGRP from DRG neurons, but it reversed the GG-induced increase in CGRP release from DRG neurons

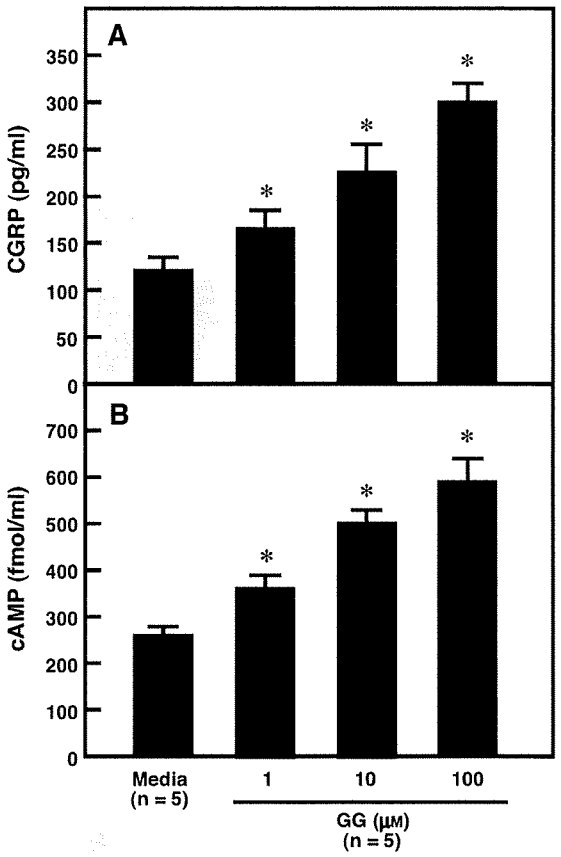

Fig. 1. Effects of α-D-Glucosylglycerol (GG) on CGRP Release from DRG Neurons (A) and Intracellular cAMP Levels in DRG Neurons (B) Isolated from WT Mice.

DRG neurons were incubated with GG (1, 10, and 100 μM) for 30 min. Supernatants were collected, and CGRP levels were measured by enzyme immunoassay. Intracellular cAMP levels were measured by enzyme immunoassay. Each value represents the mean ± SD for five experiments. $^*p < 0.01$ *vs.* media.

(Fig. 2). To determine whether PKA is involved in GG-induced stimulation of sensory neurons, we analyzed the effects of KT5720, an inhibitor of PKA, on GG-induced increases in CGRP release from DRG neurons isolated from WT mice (Fig. 2). Pretreatment with KT5720 significantly reversed the GG-induced increase in CGRP release from DRG neurons (Fig. 2).

Effect of topical application of GG on dermal levels of IGF-I in WT and CGRP−/− mice

Applied topically, 0.005% and 0.01% GG significantly increased dermal IGF-I levels 30 min after application in WT mice ($p < 0.01$) (Fig. 3). In contrast, topical application of 0.05 or 0.1% of GG did not increase dermal IGF-I levels in the WT mice (Fig. 3). Although topical application of 0.005 and of 0.01% GG increased the dermal IGF-I levels in the WT mice, it showed no such effects in the CGRP−/− mice (Fig. 3).

Changes in dermal levels of CGRP and IGF-I with time in WT mice subjected to topical application of 0.01 and 0.1% GG

The dermal levels of CGRP and IGF-I were increased in WT mice with time after topical application of 0.01% of GG (Fig. 4). In contrast, these levels were transiently

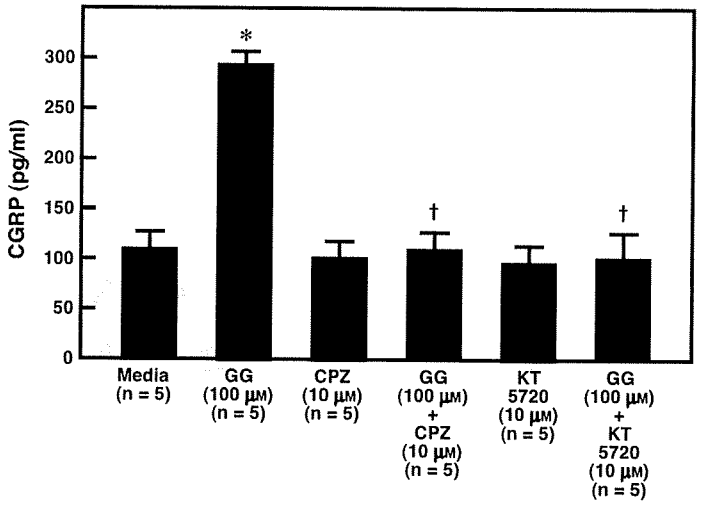

Fig. 2. Effects of α-D-Glucosylglycerol (GG) and/or Capsazepine (CPZ) or KT5720 on CGRP Release from DRG Isolated from WT Mice. DRG neurons were incubated with GG (100 μM) and/or CPZ (10 μM), an inhibitor of VR-1 activation, or KT5720 (10 μM), a PKA inhibitor, for 30 min. Each value represents the mean ± SD for five experiments. $^{*}p < 0.01$ *vs.* media. $^{\dagger}p < 0.01$ *vs.* GG.

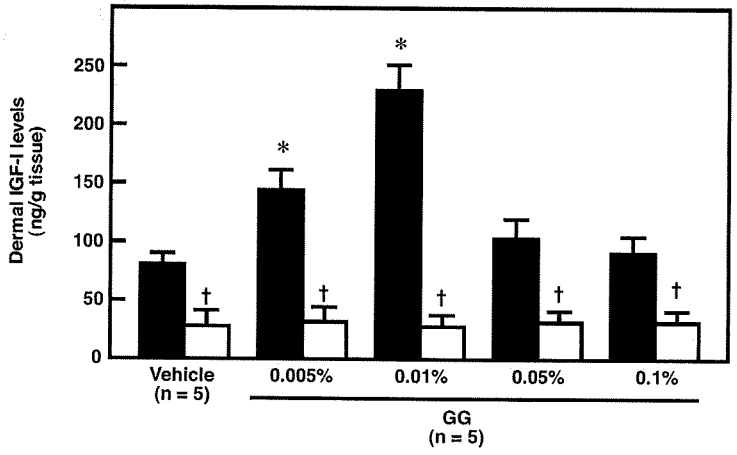

Fig. 3. Effects of Topical Application of α-D-Glucosylglycerol (GG) on Dermal IGF-I Levels in WT and CGRP−/− Mice. Skin samples were dissected 30 min after topical application of GG. Each value represents the mean ± SD for five experiments. Closed bars, WT mice; open bars, CGRP−/− mice. $^{*}p < 0.01$ *vs.* vehicle. $^{\dagger}p < 0.01$ *vs.* WT.

increased, peaking at 15 min, after topical application of 0.1% GG and decreased to baseline levels at 30 min after topical application in WT mice (Fig. 4).

Effects of 0.01% GG on dermal levels of IGF-1 mRNA and collagen in the WT and CGRP−/− mice

Topical application of 0.01% GG significantly increased dermal IGF-I mRNA levels 30 min after application in WT mice, but not in CGRP−/− mice (Fig. 5). The mean value for IGF-I/β-actin mRNA of the control in the CGRP−/− mice ($2.84 \times 10^{-4} \pm 4.94 \times 10^{-5}$; $p < 0.01$) was significantly lower than that of the control in the WT mice ($6.15 \times 10^{-4} \pm 6.71 \times 10^{-5}$).

Dermal collagen levels increased significantly 14 d after topical application of 0.01% in the WT mice ($p < 0.04$), but not in the CGRP−/− mice (Fig. 6).

Effects of topical application of 0.01% GG and vehicle on cheek skin elasticity in healthy female volunteers

To determine whether topical application of 0.01% GG would increase skin elasticity in humans, we analyzed the effects of 0.01% GG and vehicles on cheek skin elasticity in 13 and 10 healthy female volunteers respectively. Baseline data (age and cheek-skin elasticity) did not differ between the 0.01% GG group and the vehicle group (Table 1). Applied topically to the facial skin of the 13 healthy female volunteers once a day for 14 d, 0.01% GG significantly increased cheek-skin elasticity as compared with that noted before topical application ($p < 0.01$) (Fig. 7A). Topical application of vehicles did not increase cheek-skin elasticity in the remaining 10 healthy female volunteers (Fig. 7B).

Discussion

In the present study, we examined to determine whether the GG present in Japanese rice wine sake stimulates sensory neurons to increase dermal IGF-I levels in WT mice. GG increased the release of CGRP from DRG neurons isolated from WT mice. CPZ, an inhibitor of VR-1 activation, completely reversed the

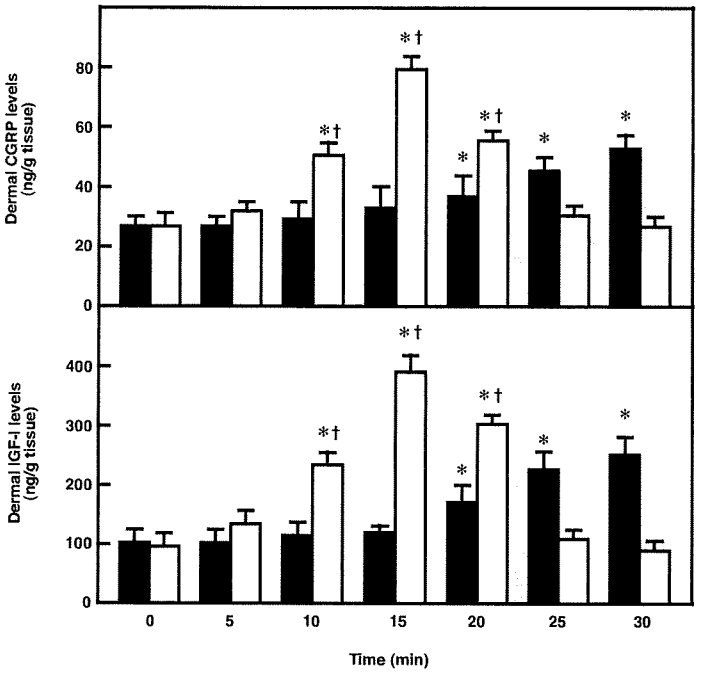

Fig. 4. Changes in Dermal Levels of CGRP and IGF-I with Time after Topical Application of 0.01 and 0.1% α-D-Glucosylglycerol (GG) in WT Mice.

Skin samples were dissected 0, 5, 10, 15, 20, 25, and 30 min after topical application of 0.01 and 0.1% GG in WT mice. Each value represents the mean ± SD for five experiments. Closed bars, 0.01% GG; open bars, 0.1% GG. $^{*}p < 0.01$ *vs.* time 0. $^{\dagger}p < 0.01$ *vs.* 0.01% GG.

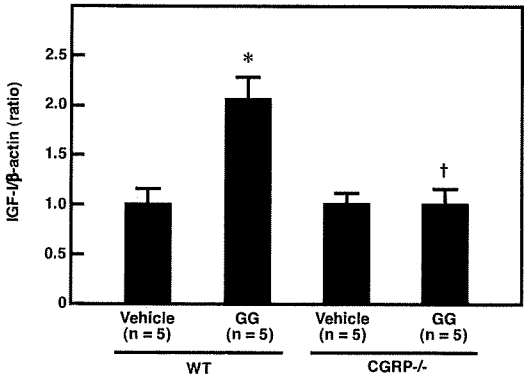

Fig. 5. Effects of Topical Application of 0.01% α-D-Glucosylglycerol (GG) on Dermal IGF-I mRNA Levels in WT and CGRP−/− Mice.

Skin samples were dissected 30 min after topical application of 0.01% GG. Each value represents the mean ± SD for five experiments. $^{*}p < 0.01$ *vs.* vehicle. $^{\dagger}p < 0.01$ *vs.* WT.

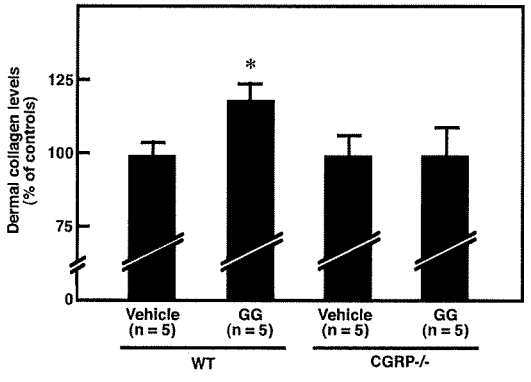

Fig. 6. Effects of Topical Application of 0.01% α-D-Glucosylglycerol (GG) on Dermal Collagen Levels in WT and CGRP−/− Mice.

Skin samples were dissected 14 d after topical application of 0.01% GG. Each value represents the mean ± SD for five experiments. $^{*}p < 0.04$ *vs.* vehicle.

GG-induced increase in CGRP release from DRG neurons, suggesting that GG increases the release of CGRP from sensory neurons *via* activation of VR-1.

We found that GG increased cAMP levels in DRG neurons isolated from WT mice. CGRP has been found to increase cAMP levels in sensory neurons, thereby sensitizing VR-1 to endogenous agonist, such as anandamide through the activation of PKA.[18,19,26] We recently reported that stimulation of sensory neurons increased tissue cAMP levels in WT mice, but not in CGRP−/− mice,[27] suggesting that CGRP plays a critical role in increases in cAMP levels in sensory neurons upon stimulation. Based on these observations, it is likely that the CGRP released from sensory neurons stimulated by GG increases cAMP levels *via* an autocrine mechanism, thereby sensitizing VR-1 through PKA activation. Consistently with this notion, a PKA inhibitor, KT5710, reversed GG-induced increases CGRP release from DRG neurons, as found in the present study.

Table 1. Baseline Data for Healthy Female Volunteers

	Vehicle (n = 10)	0.01% GG (n = 13)	*p* values
Age	36.5 ± 8.7	35.6 ± 10.7	0.834
Cheek skin elasticity	0.318 ± 0.036	0.326 ± 0.058	0.684

Values are represents mean ± SD. GG, α-D-glucosylglycerol.

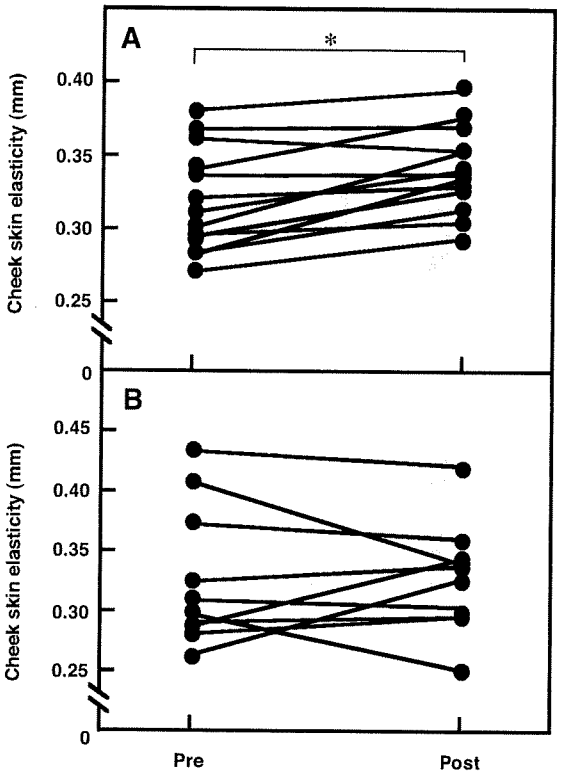

Fig. 7. Effects of Topical Application of 0.01% α-D-Glucosylglycerol (GG) (A) and Vehicle (B) on Cheek Skin Elasticity in Healthy Female Volunteers.

GG and vehicle was applied to the facial skin of 13 and 10 female volunteers respectively once a day for 14 d. Cheek skin elasticity was measured by Cutemeter before and after the experiments. $^{*}p < 0.01$ *vs.* pre.

We have reported that stimulation of sensory neurons by topical application of capsaicin increases dermal IGF-I production in WT mice,[8] suggesting that topical application of GG increases dermal IGF-I levels by stimulating sensory neurons in WT mice. Consistently with this hypothesis, topical application of 0.005 and 0.01% GG increased dermal IGF-I levels in the WT mice, but not in the CGRP−/− mice 30 min after topical application.

The dermal levels of IGF-I increase significantly 30 min after topical application of 0.01% GG, as found in the present study. Since CGRP has vasorelaxant effects,[28] it is possible that topical application of GG increases dermal tissue blood flow, thereby increasing dermal IGF-I levels. However, this possibility is less likely, since the dermal levels of IGF-I mRNA increased significantly 30 min after topical application of GG in the present study.

Since skin fibroblasts have been found to express the CGRP receptor[29] and are capable of producing IGF-I,[30] our present observations suggest that topical application of 0.01% GG increases dermal IGF-I levels in the skin fibroblasts through stimulation of sensory neurons.

Although GG increased the release of CGRP from DRG neurons isolated from the WT mice in a concentration-dependent manner *in vitro*, GG at concentrations higher than 0.05% did not increase dermal IGF-I levels in these mice 30 min after topical application. We have reported that dermal IGF-I levels increased transiently after topical application of 0.01% capsaicin in WT mice,[8] suggesting that 0.05 and 0.1% GG more strongly stimulates sensory neurons than 0.005 and 0.01% GG, thereby rapidly increasing dermal IGF-I levels at peak time points earlier than 30 min after topical application, and that these increases are followed by rapid decreases due to depletion of CGRP from the sensory neurons. Consistently with this hypothesis, the dermal levels of CGRP and IGF-I transiently increased and peaked at 15 min after topical application of 0.1% GG, and decreased to baseline levels 30 min after topical application in WT mice.

Topical application of 0.01% GG increases dermal IGF-I levels 30 min after application, as found in the present study. Production of IGF-I *via* capsaicin *in vivo* is more rapid than that in response to CGRP *in vitro*,[31] indicating that the former is not mediated by increases in transcription, as is the latter, but rather by other unknown mechanisms. Our previous study indicates that subcutaneous administration of capsaicin increases the tissue levels of IGF-I and IGF-I mRNA in various organs, including the skin, 30 min after administration in mice,[7] suggesting the possibility that stimulation of sensory neurons by topical application of 0.01% GG increases IGF-I production by increasing its transcription. This possibility should be examined in future experiments.

IGF-I increases the production of collagen[3] and elastin[32] by skin fibroblasts and promotes the proliferation of keratinocytes,[33] suggesting that IGF-I produced by fibroblasts acts on these fibroblasts themselves as well as on keratinocytes, promoting the production of collagen and elastin and the proliferation of the cells, respectively. Consistently with this hypothesis, dermal levels of collagen increased 14 d after topical application of 0.01% GG in the WT mice, but not in CGRP−/− mice as found in the present study.

Patients with Laron syndrome show skin morphological changes such as decreased thickness with decrease of the elastin content.[34] The IGF-I receptor has been found to be expressed in biopsy specimens of the human skin.[30] These observations suggest that the detrimental skin morphological changes observed in patients with Laron syndrome are attributable to reduced production of IGF-I, raising the possibility that IGF-I plays critical roles in the maintenance of skin integrity.

Topical application of 0.01% GG to facial skin significantly increased cheek skin elasticity in 13 healthy female volunteers after 14 d of application ($p < 0.01$), but topical application of the vehicles did not increase skin elasticity in the 10 healthy female volunteers. We have reported that topical application of 0.01% capsaicin increased cheek skin elasticity in healthy female volunteers.[8] These observations strongly suggest that GG increases cheek skin elasticity in healthy female volunteers by activating sensory neurons. The important mechanical property that primarily maintains skin elasticity is attributable to the content and molecular structure of the collagen fibers embedded in the ground substance.[35] Since dermal levels of collagen increased after topical application of 0.01% GG in the WT mice, it is likely that dermal levels of collagen are increased, thereby at least in part contributing to the

increase in cheek skin elasticity in the volunteers after topical application of 0.01% GG.

The sweat secretion rate has been found to be lower in patients with GH deficiency who have low serum IGF-I levels.[36] A decrease in the ability to sweat results from atrophy of the eccrine sweat glands due to a lack of stimulation by GH or IGF-I, or both.[37] Since intra-epidermal elasticity is known to be associated with the presence of sweat,[38] topical application of 0.01% GG have increased the secretion of sweat in the facial skin epidermis of the volunteers, contributing to the improved facial skin elasticity.

Although sake has been used as a skin care lotion in Japan since ancient times,[12] the precise mechanisms underlying this effect are not well understood. Increases in dermal IGF-I production induced by GG *via* sensory neuron stimulation might explain at least in part this favorable effect of sake on the skin.

References

1) Daughaday WH and Rotwein P, *Endocr. Rev.*, **10**, 68–91 (1989).
2) Tavakkol A, Varani J, Elder JT, and Zouboulis CC, *Arch. Dermatol. Res.*, **291**, 643–651 (1999).
3) Harrison CA, Gossiel F, Bullock AJ, Sun T, Blumsohn A, and Mac Neil S, *Br. J. Dermatol.*, **154**, 401–410 (2006).
4) Maggi CA and Meli A, *Gen. Pharmacol.*, **19**, 1–43 (1988).
5) Dray A, *Br. J. Anaesth.*, **75**, 125–131 (1995).
6) Rosenfeld MG, Mermod JJ, Amara SG, Swanson LW, Sawchenko PE, Rivier J, Vale WW, and Evans RM, *Nature*, **304**, 129–135 (1983).
7) Harada N, Okajima K, Kurihara H, and Nakagata N, *Neuropharmacology*, **52**, 1303–1311 (2007).
8) Harada N and Okajima K, *Growth Horm. IGF Res.*, **17**, 171–176 (2007).
9) Harada N, Okajima K, Arai M, Kurihara H, and Nakagata N, *Growth Horm. IGF Res.*, **17**, 408–415 (2007).
10) Nakahara M, Mishima T, and Hayakawa T, *Biosci. Biotechnol. Biochem.*, **71**, 427–434 (2007).
11) Kitamura N, Ota Y, Haratake A, Ikemoto T, Tanno O, and Horikoshi T, *Skin Pharmacol.*, **10**, 153–159 (1997).
12) Hirotsune M, Haratake A, Komiya A, Sugita J, Tachihara T, Komai T, Hizume K, Ozeki K, and Ikemoto T, *J. Agric. Food Chem.*, **53**, 948–952 (2005).
13) Takenaka F, Uchiyama H, and Imamura T, *Biosci. Biotechnol. Biochem.*, **64**, 378–385 (2000).
14) Mackay MA, Norton RS, and Borowitzka L, *J. Gen. Microbiol.*, **130**, 2177–2191 (1984).
15) Perkins MN and Campbell EA, *Br. J. Pharmacol.*, **107**, 329–333 (1992).
16) Oh-hashi Y, Shindo T, Kurihara Y, Imai T, Wang Y, Morita H, Imai Y, Kayaba Y, Nishimatsu H, Suematsu Y, Hirata Y, Yazaki Y, Nagai R, Kuwaki T, and Kurihara H, *Circ. Res.*, **89**, 983–990 (2001).
17) Harada N, Okajima K, Uchiba M, Kurihara H, and Nakagata N, *Thromb. Haemost.*, **95**, 788–795 (2006).
18) Mohapatra DP and Nau C, *J. Biol. Chem.*, **278**, 50080–50090 (2003).
19) Hou L and Wang X, *J. Neurosci. Res.*, **66**, 592–600 (2001).
20) Sirotkin AV, Florkovicova I, Makarevich AV, Schaeffer HJ, Kotwica J, Mamet PG, and Sanislo P, *J. Reprod. Dev.*, **49**, 141–149 (2003).
21) Geppetti P, Tramontana M, Evangelista S, Renzi D, Maggi CA, Fusco BM, and Del Bianco E, *Gastroenterology*, **101**, 1505–1511 (1991).
22) Tomomasa T, Ogawa T, Hikima A, Tabata M, Kaneko H, and Morikawa A, *J. Pediatr. Gastroenterol. Nutr.*, **34**, 169–173 (2002).
23) Junquiera LC, Junqueira LC, and Brentani RR, *Anal. Biochem.*, **94**, 96–99 (1979).
24) Joseph J, Joseph L, Shekhawat NS, Devi S, Wang J, Melchert RB, Hauer-Jensen M, and Kennedy RH, *Am. J. Physiol. Heart Circ. Physiol.*, **285**, H679–H686 (2003).
25) Sumino H, Ichikawa S, Abe M, Endo Y, Nakajima Y, Minegishi T, Ishikawa O, and Kurabayashi M, *Endocr. J.*, **51**, 159–164 (2004).
26) Schnizler K, Shutov LP, van Kanegan MJ, Merrill MA, Nichols B, McKnight GS, Strack S, Hell JW, and Usachev YM, *J. Neurosci.*, **28**, 4904–4917 (2008).
27) Zhao J, Harada N, Kurihara H, Nakagata N, and Okajima K, *Neuropharmacology*, in press.
28) Okajima K and Harada N, *Curr. Med. Chem.*, **13**, 2241–2251 (2006).
29) Hodak E, Gottlieb AB, Anzilotti M, and Krueger JG, *J. Invest. Dermatol.*, **106**, 564–570 (1996).
30) Tavakkol A, Elder JT, Griffiths CE, Cooper KD, Talwar H, Fisher GJ, Keane KM, Foltin SK, and Voorhees JJ, *J. Invest. Dermatol.*, **99**, 343–349 (1992).
31) Vignery A and McCarthy TL, *Bone*, **18**, 331–335 (1996).
32) Davidson JM, Zoia O, and Liu JM, *J. Cell. Physiol.*, **155**, 149–156 (1993).
33) Krane JF, Murphy DP, Carter DM, and Krueger JG, *J. Invest. Dermatol.*, **96**, 419–424 (1991).
34) Laron Z, *J. Clin. Endocrinol. Metab.*, **89**, 1031–1044 (2004).
35) Pierard G, "Cutaneous Investigation in Health and Disease," ed. Leveque T, Dekker, New York, pp. 215–240 (1989).
36) Pedersen SA, Welling K, Michaelsen KF, Jorgensen JO, Christiansen JS, and Skakkebaek NE, *Lancet*, **2**, 681–682 (1989).
37) Lange M, Thulesen J, Feldt-Rasmussen U, Skakkebaek NE, Vahl N, Jorgensen JO, Christiansen JS, Poulsen SS, Sneppen SB, and Juul A, *Eur. J. Endocrinol.*, **145**, 147–153 (2001).
38) Serban G, Edelberg M, Garcia M, and Hambridge A, *Bioeng. Skin*, **2**, 134 (1986).

Circulation Research
JOURNAL OF THE AMERICAN HEART ASSOCIATION

Role of Mesodermal FGF8 and FGF10 Overlaps in the Development of the Arterial Pole of the Heart and Pharyngeal Arch Arteries

Yusuke Watanabe, Sachiko Miyagawa-Tomita, Stéphane D. Vincent, Robert G. Kelly, Anne M. Moon and Margaret E. Buckingham

Circ. Res. 2010;106;495-503; originally published online Dec 24, 2009;
DOI: 10.1161/CIRCRESAHA.109.201665
Circulation Research is published by the American Heart Association. 7272 Greenville Avenue, Dallas, TX 72514
 Print ISSN: 0009-7330. Online ISSN: 1524-4571